Spurious isospin symmetry breaking in the IMSRG

Alexander Farren

2023 Naughton Fellowship REU Program
Department of Physics and Astronomy
University of Notre Dame

ADVISOR(S): Prof. Ragnar S. Stroberg

Abstract

The basics of nuclear physics and quantum many-body theory are covered with the goal of understanding the IMSRG formalism of *ab initio* nuclear many-body theory. Sources of spurious isospin symmetry breaking (ISB) in both post-Hartree-Fock IMSRG (2) and (3) truncations for a reduced orbital space ^{14}O Minnesota reference were traced back to a problematic nested commutator $\left[\eta(s), \left[\eta(s), T^2(0)\right]\right]$. The latter was reduced to an analytic sum which agreed with computational results. Asymmetric definitions of the reference state, $H^{\text{od}}(s)$ and Δ were found to spoil the isospin symmetry of the problematic term. Using Møller-Plesset partitioning of Δ in the White generator $\eta(s) \sim 1/\Delta$ or simply replacing the latter with the imaginary time generator $\eta(s) \sim \text{sgn}(\Delta)$ remedied the spurious ISB for symmetric reference and offdiagonal definitions.

Acknowledgements

Contents

⓪ Mise-en-scène

Since the 1950's, we have been developing and refining the Standard Model of particle physics by challenging theoretical predictions with increasingly precise experimental data. One such prediction is the unitarity of the Cabibbo-Kobayashi-Maskawa (CKM) matrix. The CKM matrix

$$\begin{pmatrix} |d_w\rangle \\ |s_w\rangle \\ |b_w\rangle \end{pmatrix} = \begin{pmatrix} V_{ud} & V_{us} & V_{ub} \\ V_{cd} & V_{cs} & V_{cb} \\ V_{td} & V_{ts} & V_{tb} \end{pmatrix} \begin{pmatrix} |d_s\rangle \\ |s_s\rangle \\ |b_s\rangle \end{pmatrix}$$

details the discrepancy between the weak and mass eigenstate representations of quark flavour change. In particular, the matrix element V_{ud} is of interest due to its major role in the unitarity condition

$$|V_{ud}|^2 + |V_{us}|^2 + |V_{ub}|^2 = 0.9985(05) \overset{!}{=} 1,$$

where $|V_{ud}|^2 \approx 0.97373(31)$ [1, 2]. In the context of nuclear β decay, the weak interaction is equally influenced by the polar and axial vector terms, corresponding to Fermi and Gamow-Teller decay respectively. If we consider $0^+ \to 0^+$ superallowed β Fermi decays, we can relate V_{ud} to precisely measurable coupling constants G_F and G_V as $V_{ud} = G_V/G_F$. We want to compare prediction to experiment while minimizing both sides' uncertainty.

There is a theoretical correction δ_C, to what was originally thought to be G_V, related to *isospin symmetry breaking* (ISB). Isospin was introduced as a quantum number to treat protons and neutrons as two sides of the same coin. Protons and neutrons are, however, different with respect to the Coulomb interaction and pion exchange. This means the symmetry under isospin rotation (going from a proton to a neutron or vice versa) is broken. The probability for an initial $t = 1$ nuclear state $|\psi_i\rangle$ to transition to a final state with raised or lowered isospin $|\psi_f\rangle$, e.g. via β decay, is

$$|M_{fi}|^2 = \left|\langle\psi_f|T^\pm|\psi_i\rangle\right|^2 \equiv (1 - \delta_C)\left|\langle\psi_f^{iso}|T^\pm|\psi_i^{iso}\rangle\right|^2 = 2(1 - \delta_C),$$

where the states labeled $|\psi^{iso}\rangle$ (in the isospin limit) respect isospin symmetry and are trivial to work with. Improving the reliability of IMSRG computational methods in quantifying this δ_C correction was the motivation for this research. We seek to identify and understand sources of spurious ISB.

In this text, we will cover some preliminary notions in nuclear physics and many-body theory before we discuss the IMSRG framework. I have tried to keep the sections coherent while including as much as necessary from various sources (all of which are appropriately cited).

① Nuclear Physics

This section takes from various courses on introductory nuclear physics [3–5]. Our first goal will be to understand the internuclear potential and derive the nuclear shell model from using the mean field or Hartree-Fock approximation. We will then review the basics of beta decay and isospin.

1.1 Nuclei properties

A *nuclide* $^A_Z X_N$ with *atomic number Z* and *nucleon number A* is composed of Z protons and $N = A - Z$ neutrons. The (half-way charge density) radius R of most nuclei is represented by

$$R \approx R_0 A^{\frac{1}{3}}, \tag{1.1}$$

where $R_0 = 1.2 \times 10^{-15}$ m is an experimentally determined constant. A is also the *mass number* of the nuclide, since the proton and neutron both approximately have rest mass 1 u $\approx 1.66 \times 10^{-27}$ kg (atomic mass unit, defined as 1/12 the mass of $^{12}_6$C). All nuclei have approximately the same (nucleon) density since

$$V = \frac{4}{3}\pi R^3 = \frac{4}{3}\pi R_0^3 A \implies \frac{A}{V} = \text{const.} \tag{1.2}$$

Nuclides with same Z but different A are called *isotopes*. Those with same N but different A are called *isotones* and those with same A but different Z are called *isobars*.

Nucleons are fermions with spin $s = 1/2$ so that $\hat{S}^2 = \hbar^2 s(s+1) = 3\hbar^2/4$ and $\hat{S}^z = \hbar m_s = \pm\hbar/2$. Combining the orbital and spin angular momenta of all nucleons composing a nucleus gives the *nuclear spin I*. When A is even I is an integer, when A is odd I is a half integer since the orbital angular momenta are integer numbers and the spin of each nucleon is $1/2$.

1.2 Binding energy and nuclear force

An atom's mass is *not equal* to the sum of its constituent nucleons and electrons. This is because the energy required to bind the nucleus is borrowed from the constituents as mass energy. The *mass defect Δm* associated with an atom $^A_Z X$ with mass $m(A, Z) = m(^A_Z X)$ is

$$\Delta m(A, Z) \equiv Z m_\text{p} + Z m_\text{e} + (A - Z)m_\text{n} - m(A, Z), \tag{1.3}$$

where we can usually ignore the electron mass contributions. The *binding energy* is then

$$B(A, Z) \equiv \Delta m(A, Z)c^2. \tag{1.4}$$

It's always useful to know $m_p \approx 938.3$ MeV/c^2 and $m_n \approx 939.6$ MeV/c^2. Usually $\Delta m/m \approx 0.01$. The binding energy $B(A, Z)$ is the energy required to split the nucleus into its A constitutents. B increases with A so it's useful to refer to the *binding energy per nucleon B/A*.
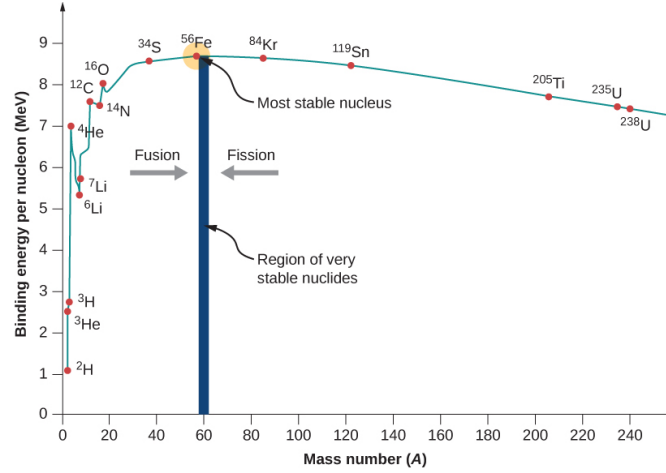
Fig. 1 Nuclei binding energy per nucleon as a function of the nuclei's mass number A [6].

Looking at Fig. 1, we see that the binding energy per nucleon increases to a maximum of 8.6 MeV around $A = 60$ and then decreases down to about 7.6 MeV. We see sharp peaks in B/A for ^{4}He, ^{8}Be, ^{12}C, ^{16}O, ^{20}Ne and ^{24}Mg. These are all multiples of the alpha particle $^4_2$He^{2+} (Helium 4 nucleus), making them more stable . We call the residual strong force between nucleons the *nuclear force*. From Fig. 2 we see that the nuclear force is

- repulsive at very short ranges ($<$ 1fm), keeping nucleons at average distance $2R_0$,
- attractive beyond this range and strong enough to overcome any Coulombic repulsion,
- short ranged to the order of R_0, nearest-neighbour binding only $\implies$ # bonds $\propto A$,
- charge independent, i.e. the same for p-p, n-n and p-n interactions,
- spin dependent and so is the binding energy.

A qualitative explanation of the B/A graph comes from the nuclear force. At low A, so for light nuclei, all nucleons are close enough to one another to experience each other's attractive nuclear force. Thus, the energy required to separate the nucleus will increase with A as for every nucleon added the original nucleons are now more tightly bound.

Conversely, at high values of A, so for heavier nuclei, every nucleon interacts with equally many neighbours since some are too far away. This is why, as A increases for heavy nuclei, B/A does not increase. In fact, it *decreases* because simultaneously more protons are being added so that the longer-ranged Coulomb force tends to repel nucleons from each other, making it easier to separate them and thus decreasing B/A. This is know as *saturation of the nuclear force*.

The Coulombic proton repulsion does not affect B/A for smaller A because the nuclear energy is about 50 times stronger at this distance (typical inter-nucleon distance).
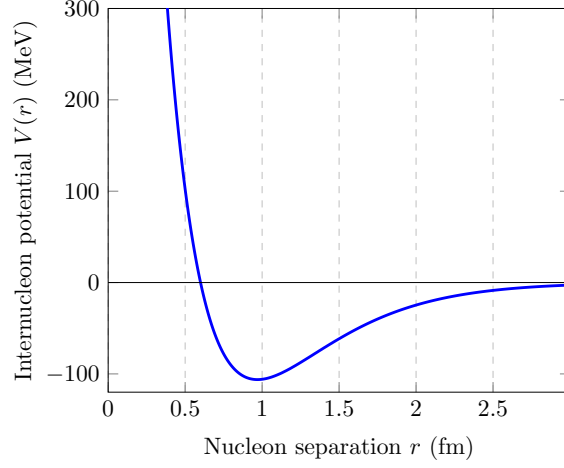
Fig. 2 Sketch of an internucleon potential with repulsive core and saturation [7].

Of the approximately 2500 known nuclei, only 270 are stable with respect to nuclear decay. The heaviest stable nuclide with $Z = N$ is $^{40}_{20}\text{Ca}$ and the heaviest of all stable nuclides is $^{208}_{82}\text{Pb}$. Stable nuclei can only be found in the *valley of stability*, between $N = Z$ and $N = 2Z$. As A increases, it's more likely that neutrons 'stick' to the nucleus since they experience no Coulombic repuslsion, in contrast with protons.

To summarise some key points about the B/A vs A plot:

- Rising trend for low A due to nuclear bonds not being fully saturated.

- Increased stability for even-even nuclei due to pairing energy (consequence of 1.4).

- Slow decrease as A increases due to increasing effect of unsaturated Coulombic proton-proton repulsion.

1.3   Shell model

Analogous to the electronic shell model for atoms, the nuclear shell model understands nucleons' states as assignments to certain energy levels, according to the quantum numbers determining the energy of the nucleon

$$E_{n\ell} = \hbar\omega(2n + \ell + \frac{3}{2}) - V_0'. \tag{1.5}$$

These energies are those of a three-dimensional harmonic oscillator in a well of depth V_0' (by construction). The shell model accurately predicts the *magic numbers* of nucleons, which corresponding to energetically stable configurations of nuclei. This section covers the development of the model as outlined in [8]. To construct this model we start with the Hamiltonian for a nucleus,

$$\hat{H} = \sum_i \frac{\hat{P}_i^2}{2m_i} + \sum_{i<j} \hat{V}_{\text{nuc}}(|\hat{X}_i - \hat{X}_j|) + \sum_{i<j}^{\text{protons}} \frac{e^2}{|\hat{X}_i - \hat{X}_j|}. \tag{1.6}$$

First, we treat the averaged field affecting each nucleon, whereby we can write the Hamiltonian as

$$\hat{H} \equiv \sum_{j}^{\text{neutrons}} \hat{H}_j^{\text{n}} + \sum_{k}^{\text{protons}} \hat{H}_k^{\text{p}}, \tag{1.7}$$

$$\hat{H}_j^{\text{n}} = \frac{\hat{P}_j^2}{2m_{\text{n}}} + \hat{V}_{\text{nuc}}^j(|\hat{X}_j|), \qquad \hat{H}_k^{\text{p}} = \frac{\hat{P}_k^2}{2m_{\text{p}}} + \hat{V}_{\text{nuc}}^k(|\hat{X}_k|) + \hat{V}_{\text{C}}^k(|\hat{X}_k|), \tag{1.8}$$

where $\hat{H}_j^{\text{n}}$ is the Hamiltonian for the neutrons with mean field

$$\hat{V}_{\text{nuc}}^j = \sum_{i<j} \hat{V}_{\text{nuc}}(|\hat{X}_i - \hat{X}_j|), \tag{1.9}$$

and $\hat{H}_k^{\text{p}}$ is the Hamiltonian for the proton with mean field

$$\hat{V}_{\text{nuc}}^k + \hat{V}_{\text{C}}^k = \sum_{i<k} \hat{V}_{\text{nuc}}(|\hat{X}_i - \hat{X}_k|) + \sum_{i<k}^{\text{protons}} \hat{V}_{\text{C}}(|\hat{X}_i - (\hat{c}X_k|). \tag{1.10}$$

These *mean fields* (1.9) & (1.10) are the potentials felt by each nucleon as a result of interacting with every other nucleon. In reality the fields affecting each nucleon depend on the others' position, so are not fixed.

We approximate the nucleon-nucleon interaction (see Fig. 2) to be a smooth well of depth V_0, determined by internuclear separation r, with an oscillator part[1]

$$V_{\text{nuc}}(r) \approx -V_0(1 - \frac{r^2}{R^2}), \tag{1.11}$$

where $R \approx 1.25A^{-1/3}$ is the familiar radius of a nucleus with mass number A (1.1). In the case of protons, which are charged, one must also add to the Hamiltonian a Coulomb interaction term, where Z is the atomic number

$$V_{\text{C}}(r) \approx \frac{(Z-1)e^2}{R}\left[\frac{3}{2} - \frac{r^2}{2R^2}\right]. \tag{1.12}$$

This is the Coulombic potential of a uniformly charged sphere, when standing inside the sphere. Of course each proton only sees $Z - 1$ other protons. This means nucleons experience an effective or mean field

$$\begin{aligned} V_{\text{eff}}(r) &= r^2\left(\frac{V_0}{R^2} - \frac{(Z-1)e^2}{2R^2}\right) - V_0 + \frac{3}{2}\frac{(Z-1)e^2}{R} \\ &\equiv \frac{1}{2}m\omega^2 r^2 - V_0', \end{aligned} \tag{1.13}$$

where the Coulombic interaction is not included in the neutron case.

---

[1]Another valid description of V_{nuc} is the Woods-Saxon potential [9].

Note the square well V_0' is shallower for protons and we define the oscillator frequencies as

$$\omega^2 \equiv \begin{cases} \left[2V_0 - (Z-1)e^2\right]/m_{\mathrm{p}}R^2 & \text{for protons,} \\ 2V_0/m_{\mathrm{n}}R^2 & \text{for neutrons.} \end{cases} \tag{1.14}$$

The energy levels of the nucleus are approximated as those of a 3D harmonic oscillator inside a well of depth V_0'.

$$E_N \approx \hbar\omega(N + \frac{3}{2}) - V_0'. \tag{1.15}$$

Had we solved the Schroödinger equation with the full radial equation, where the centrifugal term $\frac{\hbar^2}{2m}\frac{l(l+1)}{r^2}$ must appear [10], the energies would be labeled by radial number n and orbital number ℓ. Equating them to the ones above gives $N = 2n + \ell$ where we know $n = 0, 1, ..., \ell = 0, 1, ...$ and $m_\ell = -\ell, ... \ell$ in integer steps. In accordance with spectroscopic notation of the atomic orbitals, we denote $\ell = 0, 1, 2, 3, ...$ as s, p, d, f and so on. The degeneracy of E_N is

$$\sum_{\ell=N,N-2,...} (2l+1) = \frac{1}{2}(N+1)(N+2) \tag{1.16}$$

without including spin as a quantum number, and $(N+1)(N+2)$ if spin is included.

This model accurately predicts the preferred cumulative occupation numbers (magic numbers) of the $N = 0, 1$ and 2 shells but fails for higher N. This is because the present nucleon Hamiltonians ignore a crucial detail.

Spin-orbit correction

The potential associated with spin-orbit coupling in the nuclear context is

$$\frac{1}{\hbar^2}\hat{V}_{\mathrm{SO}}\hat{\boldsymbol{L}} \cdot \hat{\boldsymbol{S}}. \tag{1.17}$$

Working in the eigenbasis of $\hat{J}^2 = \hat{L}^2 + \hat{S}^2 + 2\hat{\boldsymbol{L}} \cdot \hat{\boldsymbol{S}}$ and $\hat{L}^2$ and $\hat{S}^2$ we get

$$\langle \hat{\boldsymbol{L}} \cdot \hat{\boldsymbol{S}} \rangle = \frac{\hbar^2}{2}[j(j+1) - \ell(\ell+1) - s(s+1)]. \tag{1.18}$$

Noting that $j = |\ell - s|, ..., \ell + s$ in integer steps and $s = \frac{1}{2}$, we have $j = \ell \pm \frac{1}{2}$ so that

$$V_{\mathrm{eff}}(r) \rightarrow \begin{cases} V_{\mathrm{eff}}(r) + \frac{\ell}{2}V_{\mathrm{SO}}(r) & j = \ell + 1/2, \\ V_{\mathrm{eff}}(r) - \frac{\ell+1}{2}V_{\mathrm{SO}}(r) & j = \ell - 1/2. \end{cases} \tag{1.19}$$

We can choose $V_{\mathrm{SO}}(r)$ to be negative. The spatial dependence is not that important, what matters is that the previously degenerate $n\ell$ states are now split into $n\ell j$ states. Those with ℓ and s aligned are have higher energies than those with them anti-aligned. The energy difference is $\Delta E_{n\ell} = \frac{\hbar^2}{2}(2\ell+1)$ and these two states form a doublet. Using (1.16) and including spin, $N = 0, 1, 2$ had degeneracies (possible number of states occupied for each N) of
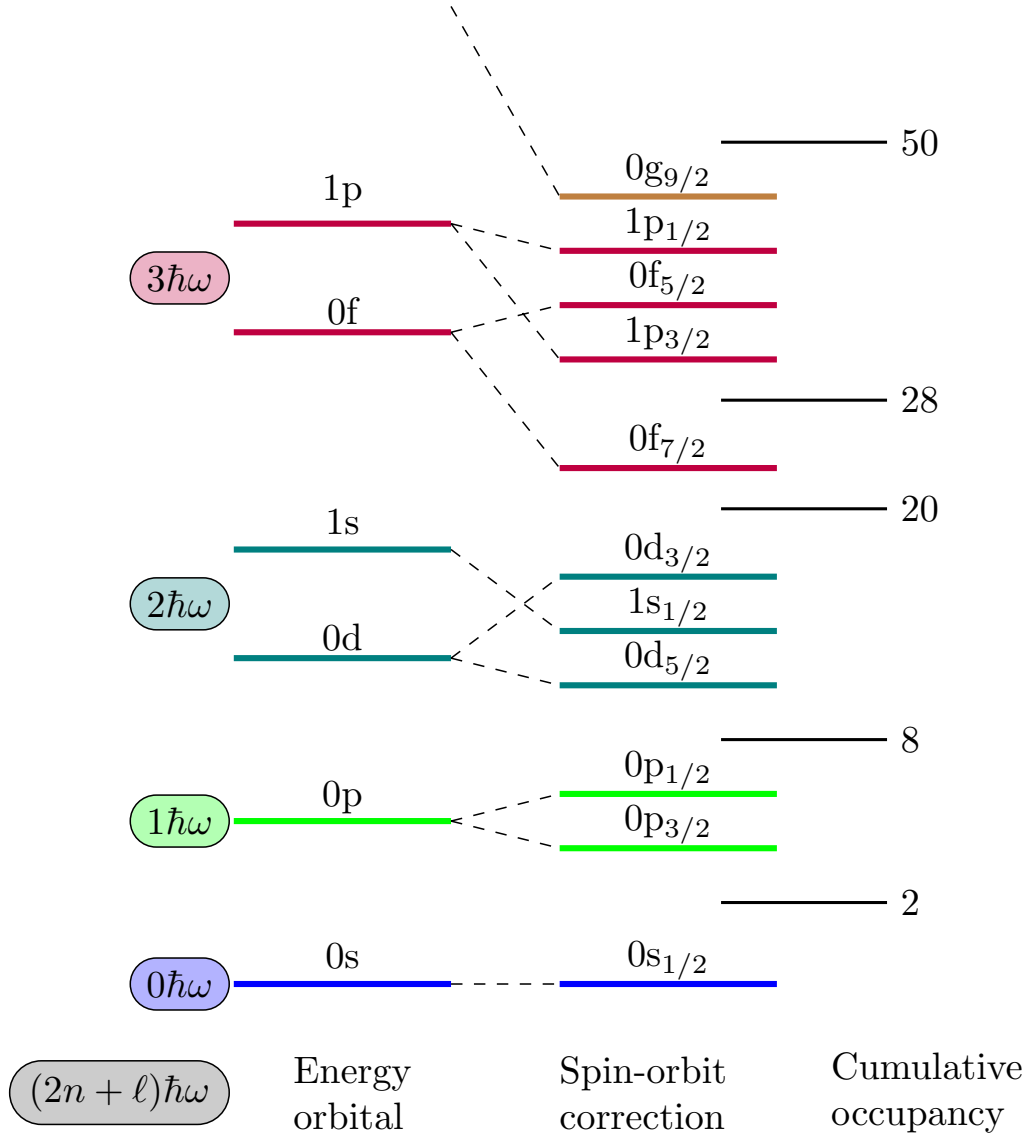
Fig. 3 Nuclear shell model

2,6 and 12 respectively. According to this simplified model, if all these shells were fully occupied, the cumulative occupancy would be 20. If we thought the next magic number would appear at $N = 3$, in agreement with the model *without* spin-orbit coupling, then the next magic number should be 40 since $N = 3$ has 20 possible sublevels. Experiment tells us the next magic number is in fact 28. Why is this?

To find the new predicted magic numbers, let us look at the $0f_{7/2}$ sublevel ($n = 0$, $\ell = 3$, $j = 7/2$). This orbital has energy 'pushed down' since the orbital and spin angular momenta of nucleons occupying this state are aligned. In fact, its energy is so low that it breaks off from the $N = 3$ shell and forms a shell of its own (Fig. 3). If you remember your angular momentum rules, you will know that m_j can take $2j + 1$ values, so $0f_{7/2}$ can be occupied by at most $2\frac{7}{2} + 1 = 8$ nucleons. Adding this to the cumulative occupancy of the first three N shells, we have retrieved the correct magic number. You can repeat this for $0g_{9/2}$ which accounts for the magic number 50 instead of 40.

$$\boxed{2, \ 8, \ 20, \ 28, \ 50, \ ...}$$

Note that the shell model is *almost* the same for the proton and neutron cases. The specific ordering of shells is determined by the various model parameters V_0, V_{SO}, $m_{n,p}$, R. Since ω depends on which nucleon type we are considering (1.14), the spacing *between* energy levels is not the same in both cases. In practice, we set both $\hbar\omega$ to the same value.

1.4 Nuclear spin and parity

In the extreme shell model, we assume that only the last unpaired nucleons dictate the properties of the nucleus. A better approximation would be to consider *all* nucleons above a filled shell as contributors. These are *valence nucleons*. Properties which are predicted by characteristics of valence nucleons include

- magnetic dipole moment,
- electric quadrupole moment,
- excited states,
- spin-parity.

In this subsection, we will briefly cover spin-parity continuing with [8]. For a more detailed discussion of why certain states are not allowed (for example odd I) see Krane [4, Ch. 3.4]. The spatial parity of a singe nucleon wavefunction is

$$\psi_{n\ell j}(x) \rightarrow \psi_{n\ell j}(-x) = (-1)^\ell \psi_{n\ell j}(x). \tag{1.20}$$

As proton and neutron shells are filled, the nucleons of each type become *paired off* yielding $s = |s_1 - s_2| = 0$ by the Pauli exclusion principle. This is because the $s = 1$ triplet is forbidden since the wavefunctions' spatial part is symmetric, since each nucleon's spatial wavefunction has parity $(-1)^\ell$ and they reside in the same ℓ orbital. (By separation of variables (1.7), we can write the combined wavefunction as the product of single-nucleon wavefunctions.) There is a *pairing force* which lowers the energy of systems with paired off nucleons.

Since nucleons get paired off, the total spin and parity of the nucleus is determined by the last *unpaired* nucleons, which necessarily reside in the highest energy levels. A nucleus can have either one valence proton, one valence neutron, or one of both unpaired.

The *parity of the nucleus* Π is the product of the parity of each valence nucleon, e.g. $(-1)^{\ell_p + \ell_n}$ if there is one valence proton and one valence neutron. Let's look at different cases for A even or odd. We will label the *spin-parity* of a nucleus/nuclide with I^Π where $\Pi = \pm$ and I is the *nuclear spin* which is either 0, a positive integer or a positive half-integer.

A **odd oe/eo**

An odd-even nucleus as an odd number of neutrons and an even number of protons. For an even-odd nucleus, it's the other way around. In both cases, A is odd. This means the nuclear spin I must be a half integer. This is because there will always be an unpaired nucleon which resides in a state $n\ell j$ and we have $I = j$ which is a positive half integer.

For example, take $^{15}_{8}\text{O}$; there is an unpaired neutron in $0p_{1/2}$, so the overall parity is $(-1)^{\ell_n} = -1$. The nuclear spin is simply j of the valence nucleon, $I = j = \frac{1}{2}$. Therefore $^{15}_{8}\text{O}$ has spin-parity $\frac{1}{2}^-$. We can find the spin-parity of any odd-A nuclide

- $^{17}_{8}\text{O}$ has $1n^0$ in $0d_{5/2} \implies \frac{5}{2}^+$,

- $^{123}_{51}\text{Sb}$ has $1p^+$ in $0g_{7/2} \implies \frac{7}{2}^+$,

- $^{29}_{14}\text{Si}$ has $1n^0$ in $1s_{1/2} \implies \frac{1}{2}^+$.

As with most rules, there are some exceptions to how nucleons fill levels

- $^{121}_{51}\text{Sb}$ has $1p^+$ in $0d_{5/2}$ (instead of $0g_{7/2}$) $\implies \frac{5}{2}^+$,

- $^{147}_{62}\text{Sn}$ has $1p^+$ in $1f_{7/2}$ (instead of $0h_{9/2}$) $\implies \frac{7}{2}^-$.

A **even**

If ee, all nucleons are paired off, meaning $I = 0$ and $\Pi = +$ always $\implies 0^+$.

If oo, there are only five stable nuclides; ^2H, ^6Li, ^{10}B, ^{14}N and $^{208}_{83}\text{Bi}$. Their spins are more complicated to calculate. Recall the nuclear spin can take values $I = |j_p + j_n|, ..., j_p + j_n$.

- Nuclei tend to have lowest spin $\implies I \sim |j_1 + j_2|$.

- Valence nucleon spins tend to align $\implies I \in \mathbb{Z}$.

Manipulating nuclear spin is the basis for magnetic resonance imagery (MRI).

1.5 Beta decay

Nuclides undergo beta decay when energetically favourable, i.e. when trending towards stable isobars (nuclides with same A). There are two types of beta decay [4];

$$\beta^- : \ n^0 \to p^+ + e^- + \bar{\nu}_e, \qquad \beta^+ : \ p^+ \to n^0 + e^+ + \nu_e. \tag{1.21}$$

We often group *electron capture* with β^+ decay as the reactions are so similar in nature.

$$p^0 + e^- \to n^0 + + \nu_e. \tag{1.22}$$

After β^-, β^+ or electron capture, the mass number A is unchanged since $Z \to Z \pm 1$ and $N \to N \mp 1$ so that $A = Z + N \to A$. *Fermi allowed* beta decays preserve the spin-parity of the parent nuclide. In particular, *super-allowed* beta decays preserve the quantum mechanical wave-function up to the exchange of a neutron for a proton or vice versa. This means the proton and neutron Fermi energies are nearly identical [5].

1.6 Isospin

Motivated by the similarity of the proton and neutron with regard to mass and their relationship with the nuclear force, a quantity was introduced by Heisenberg in 1932 to treat them as the same particle, the nucleon, with two orientations of *isospin* $t = 1/2$ [4, 11]. This paper will follow the nuclear physics convention of assigning isospin up to the neutron ($t_z = +1/2$) and down to the proton ($t_z = -1/2$). This choice is to ensure most nuclides have positive isospin projection T^z, since most nuclides have more neutrons than protons. So we assign

$$n^0 \uparrow (t_z = +\tfrac{1}{2}) \text{ isospin up} , \quad p^+ \downarrow (t_z = -\tfrac{1}{2}) \text{ isospin down}.$$

We can thus think of isospin rotation $T^\pm$ as beta decay. Isospin has all the familiar angular momentum properties

$$T^2|t\rangle = t(t+1)|t\rangle, \qquad T^\pm|t, \ t_z\rangle = \sqrt{t(t+1) - t_z(t_z \pm 1)}|t, \ t_z \pm 1\rangle, \ \dots$$

Later on, we will be focusing on ^{14}O (see Fig. 4) which has isospin $t = 1$. Let's see why that is.
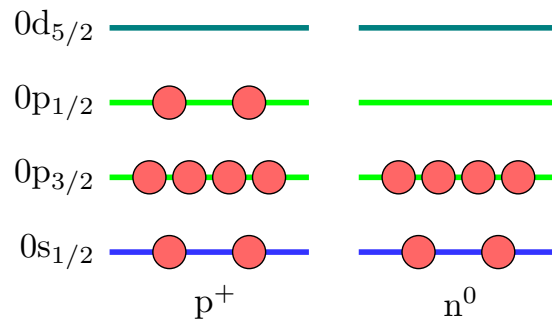
Fig. 4 The nuclear shell configuration of the ground state of ^{14}O.

If we acted on the $|^{14}\text{O}\rangle$ ground state with T^+, this would have the effect of raising the isospin of each constitutent nucleon by 1 since T is the vector sum of the constituents' isospin, only acting in their Hilbert space.

$$T^+ = \overbrace{\sum_i T_i^+}^{\text{nucleons}} = \sum_i^{\text{nucleons}} I \otimes \cdots \otimes \overbrace{T_i^+}^{i\text{th nucleon}} \otimes \cdots \otimes I. \tag{1.23}$$

Every term in the sum acting on neutrons will vanish since there is no $t_z = 3/2$ in $t = 1/2$ representation. Furthermore, every term in the sum acting on protons which occupy states symmetrically occupied by neutrons will vanish since we cannot create a second fermion in the resulting state.

The only non-zero terms in $T^+|^{14}\text{O}\rangle$ concern the two protons in $0\text{p}_{1/2}$. One application of T^+ on $|^{14}\text{O}\rangle$ creates a superposition of states where either one of the protons is a neutron. A second application of T^+ changes $|^{14}\text{O}\rangle$ to $|^{14}\text{C}\rangle$ with both protons changed to neutrons. A third application would then yield 0.

Similarly, $T^-|^{14}\text{O}\rangle = 0$. We have thus confined $|^{14}\text{O}\rangle$ to the 'bottom' triplet state $t = 1$, $t_z = -1$.

$$
\begin{aligned}
&0 \\
&|t = 1 \ t_z = +1\rangle \quad \color{red}{T^+} \\
&|t = 1 \ t_z = 0\rangle \quad \color{red}{T^+} \\
&|^{14}\text{O}\rangle \sim |t = 1 \ t_z = -1\rangle \quad \color{red}{T^+} \\
&0 \qquad\qquad\qquad \color{red}{T^-}
\end{aligned}
$$

The matrix elements of T^2 acting on a two $t = 1/2$ particle Hilbert space can be found by looking at

$$
\begin{aligned}
T^2 &= (T^z)^2 + \frac{1}{2}\left(T^+T^- + T^-T^+\right) = (T^z)^2 + I \otimes I + T_1^+ \otimes T_2^- + T_1^- \otimes T_2^+ \\
&= (T_1^z)^2 \otimes I + I \otimes (T_2^z)^2 + I \otimes I + 2T_1^z \otimes T_2^z + T_1^+ \otimes T_2^- + T_1^- \otimes T_2^+ \\
&= \underbrace{\left((T_1^z)^2 + \frac{1}{2}I\right) \otimes I + I \otimes \left((T_2^z)^2 + \frac{1}{2}I\right)}_{\text{One-particle terms}} + \underbrace{2T_1^z \otimes T_2^z + T_1^+ \otimes T_2^- + T_1^- \otimes T_2^+}_{\text{Two-particle terms}}.
\end{aligned}
\tag{1.24}
$$

By taking the one-particle or two-particle matrix elements we can find

$$T_{ij}^2 = \frac{3}{4}\delta_{ij}, \tag{1.25}$$

$$T_{ijkl}^2 = \underbrace{\frac{1}{2}\delta_{ik} \otimes \delta_{jl}}_{\text{nucleon type not changed}} + \underbrace{\delta_{i\bar{k}} \otimes \delta_{j\bar{l}}}_{p^+ \leftrightarrow n^0}.$$

where the overlined state $\bar{a}$ is identical to a but with the opposite t_z.

② Quantum Many-Body Theory

This section will mainly follow Shavitt and Bartlett [12] and [13]. When considering quantum mechanical problems with numerous independent particles, i.e. many-body problems, second quantisation provides a method for representing operators and wavefunctions compactly, and thereby manipulating them more efficiently. This is pertinent to *ab initio* nuclear theory, where a quantitative description of a collection of nucleons is desired.

2.1 Second quantisation and Fock space

We assume the existence of a one-particle basis of wavefunctions $\{\phi_i\}$ comprised of *spinorbitals* ϕ_i, such that the basis is orthonormal. The unspecified number of basis functions generate Hilbert spaces for N particles, for which basis states are tensor products of N spinorbital states (usually Hartree-Fock wavefunctions).

Because we will be dealing with nucleons, and hence fermionic states, we further assume the N-particle states are anti-symmetrised Slater determinants made up of the ϕ_i functions.

Consider the representation of a normalised *Slater determinant* (SD) wavefunction for N particles

$$|\phi_i \phi_j \dots \phi_z\rangle = |ij \dots z\rangle = \frac{1}{\sqrt{N!}} \begin{vmatrix} \phi_i(x_1) & \phi_j(x_1) & \dots & \phi_z(x_1) \\ \phi_i(x_2) & \dots & \dots & \phi_z(x_2) \\ \vdots & & & \vdots \\ \phi_i(x_N) & \dots & \dots & \phi_z(x_N). \end{vmatrix} \tag{2.1}$$

We define the *occupation number* of the ith spinorbital in the SD as

$$n_i = \begin{cases} 0 & \text{if } \phi_i \text{ not in the SD,} \\ 1 & \text{if } \phi_i \text{ is in the SD.} \end{cases} \tag{2.2}$$

The SD itself, and operators acting on it, are represented in terms of *creation* and *annihilation* operators $\hat{a}_i^\dagger$, $\hat{a}_i$ or $\hat{i}^\dagger$, $\hat{i}$ if there is no ambiguity in notation. They are defined by their action on the SD *vacuum* $|0\rangle$

$$\hat{a}_i|0\rangle = 0, \qquad \hat{a}_z^\dagger \cdots \hat{a}_i^\dagger |0\rangle = |i...z\rangle. \tag{2.3}$$

In order to comply with the anti-symmetry of states with respect to an exchange of fermions, namely $|pq\rangle = -|qp\rangle$ from (2.1), these operators satisfy

$$\left[\hat{a}_p, \hat{a}_q^\dagger\right]_+ = \hat{\delta}_{pq}, \tag{2.4}$$

$$\left[\hat{a}_p, \hat{a}_q\right]_+ = \left[\hat{a}_p^\dagger, \hat{a}_q^\dagger\right]_+ = 0,$$

where $[A, B]_+ = AB + BA$ is the anti-commutator. In particular, $\hat{a}_k | i \dots k \dots z \rangle$ and $\hat{a}_k^\dagger | i \dots z \rangle$ are found using (2.3) & (2.4). We say that the *creation operator* $\hat{a}_p^\dagger$ creates a particle in the single-particle state ϕ_p while the *annihilation operator* $\hat{a}_p$ destroys it. This is a statement that for all $N \in \mathbb{N}$, the N-body wavefunction can be generated by an application of N independent operators to a unique vacuum state. Based on (2.3) & (2.4), a definition of the *Fock space* $\mathcal{F}$ can be laid out:

- $\mathcal{F}^N \equiv \text{span}\{|i_1 \dots i_N\rangle = \hat{a}_{i_N}^\dagger \cdots \hat{a}_{i_1}^\dagger |0\rangle\}$ considering all sets of N states in a basis $B = \{\phi_i\}$.

- $\mathcal{F} \equiv \bigoplus_{N \in \mathbb{N}} \mathcal{F}^N$ where N is still the number of particles occupying non-vacuum states.

- $|\phi\rangle \in \mathcal{F} \implies |\phi\rangle = \sum_{i \in B} f_i |i\rangle + \sum_{i,j \in B} g_{ij} |ij\rangle + \sum_{i,j,k \in B} h_{ijk} |ijk\rangle + \dots$.
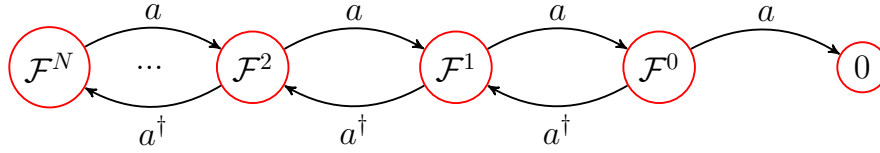
Our immediate goal is to express many-body operators in terms of creation and annihilation operators. To this end, it is convenient to expand the operators in representations of eigenstates of their single-particle counterpart and then transform to an arbitrary basis. So, we have to specify how to change between single particle bases, $\{\phi_i\} \rightarrow \{\tilde{\phi}_i\}$ and how this affects the ladder operators algebra $\{\hat{a}_i\}$.

For complete sets of states $\{\phi_i\}$ and $\{\tilde{\phi}_i\}$, $I = \sum_i |i\rangle\langle i| = \sum_{\tilde{i}} |\tilde{i}\rangle\langle \tilde{i}|$ so we get, by action on the vacuum state

$$\hat{a}_{\tilde{i}}^\dagger = \sum_i \langle i|\tilde{i}\rangle \, \hat{a}_i^\dagger \implies \hat{a}_{\tilde{i}} = \sum_i \langle \tilde{i}|i\rangle \, \hat{a}_i. \tag{2.5}$$

Alternatively, if one set of states is continuous, e.g. the position basis $|x\rangle$, $I = \int dx |x\rangle\langle x|$ so that

$$\hat{a}_i = \int dx \, \langle i|x\rangle \, \hat{a}(x), \qquad \hat{a}(x) = \sum_i \langle x|i\rangle \, \hat{a}_i. \tag{2.6}$$

In the case of a finite position space, for example $x \in [0, L]$, the momentum is discretised and the position and momentum bases are related by Fourier transform [14, pg. 103].

Symmetric one-body (1B) operators $\hat{\mathcal{O}}_1$ acting in an N-particle Hilbert space $\mathcal{F}^N$ take the form

$$\hat{\mathcal{O}}_1 = \sum_{i=1}^N \hat{o}_i, \tag{2.7}$$

where $\hat{o}_i = \overbrace{I \otimes \cdots \otimes \hat{o}_i \otimes \cdots \otimes I}^{i\text{th position}}$ acts exclusively in the ith particle's Hilbert space. For example, the total kinetic energy operator $T = \sum_i \hat{P}_i^2 / 2m_i$ and the total spin operator $\hat{S} = \sum_i \hat{S}_i$.

Define the *(occupation) number operator* $N_\lambda \equiv \hat{a}_\lambda^\dagger \hat{a}_\lambda$ such that

$$N_\lambda (\hat{a}_\lambda^\dagger)^n |0\rangle = n(\hat{a}_\lambda^\dagger)^n |0\rangle, \quad \text{or} \quad N_\lambda |\lambda_1 ... \lambda_N\rangle = n_\lambda |\lambda_1 ... \lambda_N\rangle. \tag{2.8}$$

This can be seen using the relation $\hat{a}_\lambda \hat{a}_{\lambda_N}^\dagger = \delta_{\lambda \lambda_N} - a_{\lambda_N}^\dagger \hat{a}_\lambda$, so

$$
\begin{aligned}
(\hat{a}_\lambda^\dagger \hat{a}_\lambda)\hat{a}_{\lambda_N}^\dagger \cdots \hat{a}_{\lambda_1}^\dagger |0\rangle &= \delta_{\lambda \lambda_N} |\lambda_1 ... \lambda_N\rangle + \delta_{\lambda \lambda_{N-1}} |\lambda_1 ... \lambda_N\rangle + ... + \delta_{\lambda \lambda_1} |\lambda_1 ... \lambda_N\rangle \\
&\quad + (-1)^N \hat{a}_\lambda^\dagger \hat{a}_{\lambda_N}^\dagger \cdots \hat{a}_{\lambda_1}^\dagger \hat{a}_\lambda |0\rangle \\
&= (\sum_{i=1}^N \delta_{\lambda \lambda_i}) |\lambda_1 ... \lambda_N\rangle = n_\lambda |\lambda_1 ... \lambda_N\rangle.
\end{aligned}
\tag{2.9}
$$

Consider $\hat{\mathcal{O}}_1$ with single-particle equivalent $\hat{o}$ where $|\lambda_i\rangle$ are the orthonormal eigenvectors of $\hat{o}$ with eigenvalues o_i.

$$\langle \lambda_1' ... \lambda_N' | \hat{\mathcal{O}}_1 | \lambda_1 ... \lambda_N \rangle = \langle \lambda_1' ... \lambda_N' | \sum_{i=1}^N o_{\lambda_i} | \lambda_1 ... \lambda_N \rangle = \langle \lambda_1' ... \lambda_N' | \sum_\lambda n_\lambda o_\lambda | \lambda_1 ... \lambda_N \rangle, \tag{2.10}$$

which holds for all sets of N states $\{\lambda_i\}$, We obtain the *second quantisation representation*

$$\hat{\mathcal{O}}_1 = \sum_\lambda o_\lambda N_\lambda = \sum_\lambda \langle \lambda | \hat{o} | \lambda \rangle \hat{a}_\lambda^\dagger \hat{a}_\lambda. \tag{2.11}$$

By transforming to a general basis $\{\mu\}$ using (2.5) (not necessarily eigenbasis of $\hat{o}$), we get

$$\hat{\mathcal{O}}_1 = \sum_{\mu\nu} \langle \mu | \hat{o} | \nu \rangle \hat{a}_\mu^\dagger \hat{a}_\nu. \tag{2.12}$$

Formally, $\hat{\mathcal{O}}_1$ scatters a particle from state $|\nu\rangle$ to a state $|\mu\rangle$ with probability $|\langle \mu | \hat{o} | \nu \rangle|^2$. For example take a collection of spin-1/2 particles, then the ith particle's spin operator in the spin state basis $\{\uparrow, \downarrow\}$ can be represented with the Pauli matrices

$$\hat{S}_i = \frac{\hbar}{2}\sigma \implies \hat{s}_i^z = \frac{\hbar}{2}\begin{pmatrix} 1 & 0 \\ 0 & -1 \end{pmatrix}, \quad \hat{s}_i^+ = \hat{s}_i^x + \hat{s}_i^y = \hbar\begin{pmatrix} 0 & 1 \\ 0 & 0 \end{pmatrix}. \tag{2.13}$$

This means the *total spin* operator of a collection of fermions can be rewritten [13]

$$\hat{S} \overset{(2.12)}{=} \sum_{\lambda\alpha\alpha'} \hat{a}_{\lambda\alpha}^\dagger \hat{s}_{\alpha\alpha'} \hat{a}_{\lambda\alpha'} \implies \hat{S}^z = \frac{\hbar}{2} \sum_\lambda N_{\lambda\uparrow} - N_{\lambda\downarrow}, \quad \hat{S}^+ = \hbar \sum_\lambda \hat{a}_{\lambda\uparrow}^\dagger \hat{a}_{\lambda\downarrow}, \tag{2.14}$$

where α, α' can take values $\uparrow, \downarrow$ and λ represents the rest of the quantum numbers describing the system (e.g. position, orbital angular momentum). Clearly $\hat{S}^z$ counts the net spin projection and $\hat{S}^+$ destroys particles in the spin-down before subsequently creating them in the spin-up state.

Similarly, we can derive the second quantisation representation of symmetric two-nucleon operators

$$\hat{\mathcal{O}}_2 = \sum_{\mu<\nu}^{N} \hat{o}_{\mu\nu} = \frac{1}{2} \sum_{\mu\neq\nu}^{N} \hat{o}_{\mu\nu} = ... = \frac{1}{2} \sum_{pqrs} \langle pq|\hat{o}|rs\rangle \hat{a}_p^\dagger \hat{a}_q^\dagger \hat{a}_s \hat{a}_r. \tag{2.15}$$

For example, if we consider the Hamiltonian describing a nucleus (and ignore the $3N$ force), we could write it as a sum of the free nucleon Hamiltonians $\hat{h}_i = \hat{P}_i^2/2m_i$ and the interaction terms $\hat{v}_{ij}$. Here, we sum over all nucleons

$$\hat{H} = \sum_i^N \hat{h}_i + \frac{1}{2} \sum_{i\neq j}^N \hat{v}_{ij}, \tag{2.16}$$

or, in second quantised form, where the summation indices now refer to a basis of single nucleon spinorbitals

$$\hat{H} = \sum_{pq} h_{pq} \hat{p}^\dagger \hat{q} + \frac{1}{2} \sum_{pqrs} v_{pqrs} \hat{p}^\dagger \hat{q}^\dagger \hat{s} \hat{r}. \tag{2.17}$$

2.2 Particle-hole formulation

Because nucleons fill up energy levels progressively (see 1.3), it will be convenient to define a *reference state* $|\Phi_0\rangle$ in which the nucleus is in its ground state. This means there is an energy below which all proton states are filled, and an equivalent energy for neutrons. We can think of these as Fermi energies and thus think of our fixed reference state $|\Phi_0\rangle$ as the *Fermi vacuum*. All spinorbitals which are occupied/filled in the reference are called *hole states*
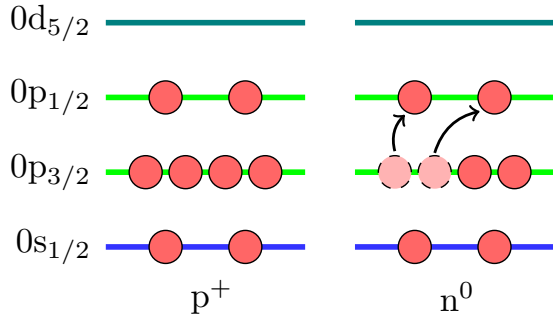
Fig. 5 An ^{14}O reference $|\Phi_0\rangle$ being excited to a possible double excitation $|\Phi_{ij}^{ab}\rangle$. The $0p_{1/2}$ state was originally a hole state for protons but a particle state for neutrons. Only excitations which conserve spin-parity I^Π are physically allowed.

and, conversely, those which are vacant/empty in the reference are called *particle states*. From now on, to indicate hole states we will use indices $i, j, k, ...$and particle states will be labelled with $a, b, c, ...$ To refer to any generic spinorbital, we will use $p, q, r, s, ...$ Reflecting how it would be unphysical to create a particle in an occupied fermionic state, or destroy a particle in an empty one, we can use the commutation relations to show

$$\hat{i}^\dagger|\Phi_0\rangle = \hat{a}|\Phi_0\rangle = 0, \qquad \langle\Phi_0|\hat{i} = \langle\Phi_0|\hat{a}^\dagger = 0. \tag{2.18}$$

Because $\hat{a}^\dagger\hat{i}$ has the effect of 'displacing' one particle, it is the basis for one-body (1B) operators. Similarly, $\hat{a}^\dagger\hat{b}^\dagger\hat{j}\hat{i}$ is a 2B operator and so on. This is known as the operator's *particle rank*.

We define other SDs relative to the reference by super/subscripting the change

$$|\Phi_i^a\rangle \equiv \hat{a}^\dagger \hat{i}|\Phi_0\rangle \qquad \text{(single excitation)}, \tag{2.19}$$

$$|\Phi_{ij}^{ab}\rangle \equiv \hat{a}^\dagger \hat{b}^\dagger \hat{j}\hat{i}|\Phi_0\rangle \quad \text{(double excitation)},$$

$$|\Phi_i\rangle \equiv \hat{i}|\Phi_0\rangle \qquad \text{(nucleon removal)},$$

$$|\Phi^a\rangle \equiv \hat{a}^\dagger|\Phi_0\rangle \qquad \text{(nucleon attachment)}.$$

The commutation relations (2.4) also mean that $\hat{i}\hat{j} = -\hat{j}\hat{i}$ so that

$$|\Phi_{ij}^{ab}\rangle = -|\Phi_{ji}^{ab}\rangle = |\Phi_{ji}^{ba}\rangle = -|\Phi_{ij}^{ba}\rangle. \tag{2.20}$$

Together with (2.19), they lead to orthonormality of this basis of SDs, i.e.

$$\langle\Phi_0|\Phi_i^a\rangle = \langle\Phi_0|\Phi_{ij}^{ab}\rangle = \ldots = 0, \qquad \langle\Phi_{i'}^{a'}|\Phi_i^a\rangle = \delta_{ii'}\delta_{aa'}, \quad \ldots \tag{2.21}$$

The energy of some reference state $|\Phi_0\rangle = |ijk...n\rangle$ can be computed by using (2.17)

$$E_0 = \langle\Phi_0|\hat{H}|\Phi_0\rangle \tag{2.22}$$

$$= \sum_{pq} h_{pq}\langle ijk...n|\hat{p}^\dagger\hat{q}|ijk...n\rangle + \frac{1}{2}\sum_{pqrs} v_{pqrs}\langle ijk...n|\hat{p}^\dagger\hat{q}^\dagger\hat{s}\hat{r}|ijk...n\rangle$$

$$= \sum_{l} h_{ll}\langle ijk...n|\hat{l}^\dagger\hat{l}|ijk...n\rangle + \frac{1}{2}\sum_{l\neq m} v_{lmml}\langle ijk...n|\hat{l}^\dagger\hat{m}^\dagger\hat{m}\hat{l}|ijk...n\rangle$$

$$+ \frac{1}{2}\sum_{l\neq m} v_{lmlm}\langle ijk...n|\hat{l}^\dagger\hat{m}^\dagger\hat{l}\hat{m}|ijk...n\rangle.$$

We get to this step for the first term by noticing that $p \neq q$ leads to zero by orthonormality, and that only hole states have non-vanishing occupation numbers . For the second term, we employ similar arguments but we also have two distinct ways of ending up with the same bra and ket by left action of the creation operators and right action of the annihilation operators respectively. The cases are when $\hat{s}$ and $\hat{p}$ are the same or when $\hat{s}$ and $\hat{q}$ are the same. (Of course, we sum over $l \neq m$ since a nucleon state cannot be destroyed twice.) Since we are summing over *all* spinorbitals, both cases appear. Noticing that $\hat{l}^\dagger\hat{l}|\Phi_0\rangle = |\Phi_0\rangle$ by definition of a hole state, and that $\hat{l}\hat{m}\hat{l}\hat{m} = -\hat{l}\hat{m}\hat{m}\hat{l}$,

$$E_0 = \sum_{l} h_{ll} + \frac{1}{2}\sum_{l\neq m} \langle lm|\hat{v}|lm\rangle_{\text{A}}. \tag{2.23}$$

We denote the *anti-symmetrised matrix element* by[2] $\langle lm|\hat{v}|lm\rangle_{\text{A}} \equiv \langle lm|\hat{v}|lm\rangle - \langle lm|\hat{v}|ml\rangle$. All operator matrix elements will be anti-symmetrised going forward (except of course for single-particle matrix elements).

---

[2]Sometimes also written as $\langle lm||lm\rangle$ when referring to the Hamiltonian two-body potential.

2.3 Normal ordering

To make use of our starting point, the reference state, we have found a compact way to write SDs by treating them as deviations. We will now work toward accomplishing the same thing for second-quantised operators.

A string of creation and/or annihilation operators is said to be *normal ordered* with respect to a reference state if all operators which destroy the state (e.g. $\hat{i}^\dagger$, $\hat{a}$) are to the right of all those which do not (e.g. $\hat{i}$, $\hat{a}^\dagger$). In the case of the physical vacuum state $|0\rangle$, a string of operators would be normal ordered if all annihilation operators were to the right. We denote a string of normal ordered operators by curly brackets[3] $\{\cdots\}$. According to Wick's theorem, we could equivalently define normal ordering with respect to $|\Phi_0\rangle$ as

$$\{\hat{p}^\dagger \hat{q}^\dagger \cdots \hat{s}\hat{r}\} \equiv \hat{p}^\dagger \hat{q}^\dagger \cdots \hat{s}\hat{r} - \langle\Phi_0|\hat{p}^\dagger \hat{q}^\dagger \cdots \hat{s}\hat{r}|\Phi_0\rangle. \tag{2.24}$$

This would of course imply $\langle\Phi_0|\{\hat{p}^\dagger \hat{q}^\dagger \cdots \hat{s}\hat{r}\}|\Phi_0\rangle = 0$ as desired. The reference state expectation value of a pair of creation and/or annihilation operators is called a *(Wick) contraction*

$$\overset{\frown}{\hat{p}^\dagger \hat{q}} \equiv \langle\Phi_0|\hat{p}^\dagger \hat{q}|\Phi_0\rangle = \hat{p}^\dagger \hat{q} - \{\hat{p}^\dagger \hat{q}\}. \tag{2.25}$$

The only *non-zero* contractions are then $\overset{\frown}{\hat{i}^\dagger \hat{j}} = \delta_{ij}$ and $\overset{\frown}{\hat{a}\hat{b}^\dagger} = \delta_{ab}$.

We are now ready to write operators relative to the reference. For example, we can write the intrinsic A-nucleon Hamiltonian, this time including both the NN and $3N$ forces [15, Ch. 10]

$$\hat{H} = (1 - \frac{1}{A})\sum_{i=1}^{A} \hat{h}_i + \frac{1}{A}\sum_{i<j}^{A} \hat{h}_{ij} + \sum_{i<j}^{A} \hat{v}_{ij} + \sum_{i<j<k}^{A} \hat{v}_{ijk}, \tag{2.26}$$

where the nucleon 1B and 2B kinetic energy terms are

$$\hat{h}_i = \hat{\boldsymbol{P}}_i^2/2m, \qquad \hat{h}_{ij} = -\hat{\boldsymbol{P}}_i \cdot \hat{\boldsymbol{P}}_j/m. \tag{2.27}$$

Now we can normal order $\hat{H}$ with respect to the a reference $|\Phi_0\rangle$. We get

$$\hat{H} = E_0 + \sum_{pq} f_{pq}\{\hat{p}^\dagger \hat{q}\} + \frac{1}{4}\sum_{pqrs} \Gamma_{pqrs}\{\hat{p}^\dagger \hat{q}^\dagger \hat{s}\hat{r}\} + \frac{1}{36}\sum_{ijklmn} W_{ijklmn}\{\hat{i}^\dagger \hat{j}^\dagger \hat{k}^\dagger \hat{n}\hat{m}\hat{l}\}, \tag{2.28}$$

where $E_0 = \langle\Phi_0|\hat{H}|\Phi_0\rangle$ is the reference state energy and f_{pq}, Γ_{pqrs} and W_{ijklmn} are anti-symmetrised matrix elements which can be found using (2.12) & (2.24) and comparing (2.26) to (2.28). These expressions are in [15, Ch. 10]. We have learned how to go from operators (acting in a particle's Hilbert space) to second-quantised operators (acting in a Fock space) to normal ordered second-quantised operators.

$$\hat{H} = \sum_{pq} h_{pq}\hat{p}^\dagger \hat{q} + \frac{1}{4}\sum_{pqrs} V_{pqrs}\hat{p}^\dagger \hat{q}^\dagger \hat{s}\hat{r} + ... = E_0 + \sum_{pq} f_{pq}\{\hat{p}^\dagger \hat{q}\} + \frac{1}{4}\sum_{pqrs} \Gamma_{pqrs}\{\hat{p}^\dagger \hat{q}^\dagger \hat{s}\hat{r}\} + ... \tag{2.29}$$

---

[3]Somtimes denoted with colons $:\cdots:$

2.4 Wick's theorem

See [15, Ch.10] for a full treatment of this subsection. The statement of Wick's theorem is that, using (2.4) and (2.24), one can recursively find

$$
\begin{aligned}
\hat{p}_1^\dagger \cdots \hat{p}_N^\dagger \hat{q}_N \cdots \hat{q} = {} & \{\hat{p}_1^\dagger \cdots \hat{p}_N^\dagger \hat{q}_N \cdots \hat{q}_1\} \\
& + \wick{\hat{p}_1^\dagger \hat{q}_1} \{\hat{p}_2^\dagger \cdots \hat{p}_N^\dagger \hat{q}_N \cdots \hat{q}_2\} - \wick{\hat{p}_1^\dagger \hat{q}_2} \{\hat{p}_2^\dagger \cdots \hat{p}_N^\dagger \hat{q}_N \cdots \hat{q}_1\} + \text{ singles} \\
& + \left(\wick{\hat{p}_1^\dagger \hat{q}_1} \wick{\hat{p}_2^\dagger \hat{q}_2} - \wick{\hat{p}_1^\dagger \hat{q}_2} \wick{\hat{p}_2^\dagger \hat{q}_1} \right) \{\hat{p}_3^\dagger \cdots \hat{p}_N^\dagger \hat{q}_N \cdots \hat{q}_3\} + \text{ doubles} \\
& + \dots + \text{ full contractions,}
\end{aligned}
\tag{2.30}
$$

where singles and doubles refer to the number of contractions in a term. Two important consquences follow by inductive reasoning, starting from (2.24)

$$
\{\cdots \hat{p}^\dagger \hat{q} \cdots\} = -\{\cdots \hat{q} \hat{p}^\dagger \cdots\},
\tag{2.31}
$$

$$
\langle \Phi_0 | \{\hat{p}^\dagger \hat{q}^\dagger \cdots \hat{s} \hat{r}\} | \Phi_0 \rangle = 0.
\tag{2.32}
$$

A less immediate consequence is related to the commutator of normal ordered operators. Take $\hat{A}$ with particle rank M and $\hat{B}$ with particle rank N, then

$$
\left[\hat{A}^{[M]}, \hat{B}^{[N]} \right] = \sum_{k=|M-N|}^{M+N-1} \hat{C}^{[k]},
\tag{2.33}
$$

which gives a sum of different kB operators $\hat{C}^{[k]}$.

2.5 Hartree-Fock equation

While deriving the shell model in 1.3, we employed the idea of a mean field experienced by each nucleon. This concept stems from Hartree-Fock theory, where we rearrange the Hamiltonian as follows [5, 12]. We can write

$$
\hat{H} = \sum_{pq} h_{pq} \hat{p}^\dagger \hat{q} + \frac{1}{4} \sum_{pqrs} \langle pq | \hat{v} | rs \rangle_{\text{A}} \hat{p}^\dagger \hat{q}^\dagger \hat{s} \hat{r} = \hat{F} + \hat{V}.
\tag{2.34}
$$

We define the *Fock operator* $\hat{F}$ in terms of an auxiliary 1B operator $\hat{U}$.

$$
\hat{F} = \sum_{pq} f_{pq} \hat{p}^\dagger \hat{q} \equiv \sum_{pq} h_{pq} \hat{p}^\dagger \hat{q} + \hat{U}.
\tag{2.35}
$$

The *residual interaction* must then be

$$
\hat{V} \equiv \frac{1}{4} \sum_{pqrs} \langle pq | \hat{v} | rs \rangle_{\text{A}} \hat{p}^\dagger \hat{q}^\dagger \hat{s} \hat{r} - \hat{U}.
\tag{2.36}
$$

In essence, $\hat{F}$ is the sum of the 1B Hamiltonians each with a mean field to be expressed by $\hat{U}$.

$$\hat{U} = \sum_{pq} u_{pq} \hat{p}^\dagger \hat{q}, \qquad u_{pq} \equiv \sum_i \langle pi|\hat{v}|qi\rangle_{\mathrm{A}}. \tag{2.37}$$

You can see that the matrix element u_{pq} is a sum over all hole states, giving us an average of the fields exerted by all other nucleons present. (Since $|qi\rangle = 0$ whenever $q = i$.) This is exactly what we had in (1.9)& (1.10). We can diagonalise $\hat{F}$ and find the Hartree-Fock eigenbasis $\{\alpha\}$ such that we get the Hartree-Fock equation

$$\varepsilon_\alpha \delta_{\alpha\beta} = h_{\alpha\beta} + \sum_i \langle \alpha i|\hat{v}|\beta i\rangle_{\mathrm{A}}, \tag{2.38}$$

and ε_α is the Hartree-Fock single-particle energy of the spinorbital ϕ_α. Note that the Hartree-Fock ground state energy is then the sum of all hole state energies. The HF eigenfunctions $\phi_\alpha(\boldsymbol{x}) = \langle \boldsymbol{x}|\alpha\rangle$ are expanded in terms of some basis, for example the harmonic oscillator. We are seeking solutions to (2.38) of the form

$$|\alpha\rangle = \sum_j C_j^\alpha |j\rangle, \qquad \hat{F}|\alpha\rangle = \varepsilon_\alpha |\alpha\rangle. \tag{2.39}$$

This eventually yields the iterative self-consistency solution

$$f_{jj'} = h_{jj'} + \sum_\beta^{\text{holes}} \sum_{j_1 j_2} \left(C_{j_1}^\beta\right)^* \langle j j_1|\hat{v}|j' j_2\rangle_{\mathrm{A}} C_{j_2}^\beta. \tag{2.40}$$

The 1B part of the original Hamiltonian $\hat{h}$ is just the kinetic energy of a single nucleon. The 2B part $\hat{v}$ contains the NN interaction and the exchange force. We can express (2.38) in position space as

$$-\frac{\hbar^2}{2m}\nabla^2 \phi_\alpha(\boldsymbol{x}) + \hat{U}\phi_\alpha(\boldsymbol{x}) = \varepsilon_\alpha \phi_\alpha(\boldsymbol{x}). \tag{2.41}$$

The mean field potential $\hat{U}$ is defined by its action on spinorbitals ϕ_α

$$\hat{U}\phi_\alpha(\boldsymbol{x}) = \hat{v}_{\mathrm{H}}\phi_\alpha(\boldsymbol{x}) - \int d^3 r' \hat{v}_{\mathrm{F}}(\boldsymbol{x}',\boldsymbol{x})\phi_\alpha(\boldsymbol{x}). \tag{2.42}$$

We have introduced the Hartree and Fock potentials $\hat{v}_{\mathrm{H}}$ and $\hat{v}_{\mathrm{F}}$

$$\hat{v}_{\mathrm{H}} = \sum_\beta^{\text{holes}} \int d^3 r' \phi_\beta^*(\boldsymbol{x}')\hat{v}(\boldsymbol{x}',\boldsymbol{x})\phi_\beta(\boldsymbol{x}), \tag{2.43}$$

$$\hat{v}_{\mathrm{F}} = \sum_\beta^{\text{holes}} \phi_\beta^*(\boldsymbol{x}')\hat{v}(\boldsymbol{x}',\boldsymbol{x})\phi_\beta(\boldsymbol{x}), \tag{2.44}$$

corresponding to the internucleon interaction and exchange force respectively.

2.6 Hamiltonian partitioning

In perturbation theory, we consider the Hamiltonian to be split up into the unperturbed or *zero-order* Hamiltonian $\hat{H}_0$ and a perturbation $\lambda \hat{V}$ where $\lambda \ll 1$. This is what is meant by *partitioning* the Hamiltonian.

$$\hat{H} \equiv \hat{H}_0 + \lambda \hat{V}. \tag{2.45}$$

We usually know the spectrum of $\hat{H}_0$

$$\hat{H}_0 |n^{(0)}\rangle = E_n^{(0)} |n^{(0)}\rangle. \tag{2.46}$$

We want to solve $\hat{H}|n\rangle = E_n |n\rangle$. By expanding E_n and $|n\rangle$ in orders of λ

$$E_n = E_n^{(0)} + \lambda E_n^{(1)} + \lambda^2 E_n^{(2)} + \dots, \tag{2.47}$$

$$|n\rangle = |n^{(0)}\rangle + \lambda |n^{(1)}\rangle + \lambda^2 |n^{(2)}\rangle + \dots . \tag{2.48}$$

By comparing terms with the same degree in λ, we find

$$E_n^{(2)} = \sum_{m \neq n} \frac{|V_{nm}|^2}{E_n^{(0)} - E_m^{(0)}}. \tag{2.49}$$

This kind of *energy denominator* $\Delta \sim E_n^{(0)} - E_m^{(0)}$ shows up in perturbation theory. As we can see the definition of Δ relies on the spectrum of $\hat{H}_0$, and so depends on how we partition the Hamiltonian.

Møller-Plesset partitioning

We can impose $\hat{H}_0 = \sum_p \varepsilon_p \hat{p}^\dagger \hat{p}$ in some single-particle basis $\{\phi_i\}$. Using (2.4) we get

$$\hat{H}_0 |rst \dots\rangle = (\varepsilon_r + \varepsilon_s + \varepsilon_t + \dots)|rst \dots\rangle, \tag{2.50}$$

which tells us that the spectrum of $\hat{H}_0$ is any SD $|rst \dots\rangle$ made up of spinorbitals $\{\phi_i\}$. If the reference is $|\Phi_0\rangle = |jk \dots n\rangle$, then

$$\hat{H}_0 |\Phi_0\rangle = E_0^{(0)} |\Phi_0\rangle, \qquad E_0^{(0)} = \varepsilon_j + \varepsilon_k + \dots + \varepsilon_n = \sum_i \varepsilon_i. \tag{2.51}$$

Note $E_0 \neq E_0^{(0)}$. In fact, $E_0 = (E_0^{(0)} + \sum_i h_{ii})/2$ using (2.23). For any other SD $|\Phi_{ij\dots}^{ab\dots}\rangle$, we then have

$$\hat{H}_0 |\Phi_{ij\dots}^{ab\dots}\rangle = (E_0^{(0)} + \varepsilon_a + \varepsilon_b + \dots - \varepsilon_i - \varepsilon_j - \dots)|\Phi_{ij\dots}^{ab\dots}\rangle. \tag{2.52}$$

In canonical Hartree-Fock theory, the 1B part of the normal ordered Hamiltonian (2.28) satisfies $f_{pq} = \varepsilon_p \delta_{pq}$. This yields

$$\hat{H}_0 |\Phi_{ij\dots}^{ab\dots}\rangle = (E_0^{(0)} + f_{aa} + f_{bb} + \dots - f_{ii} - f_{jj} - \dots)|\Phi_{ij\dots}^{ab\dots}\rangle, \tag{2.53}$$

which is often referred to as *Møller-Plesset (MP)* partitioning where $\hat{H}_0$ is the diagonal part of $\hat{F}$ in (2.35).

Epstein-Nesbet partitioning

Other partitionings of the Hamiltonian can also be used. In particular, the diagonal part of the Hamiltonian in any convenient Hilber-space representation can be used as the zero-order Hamiltonian. For a generic basis $\{\Phi_i\}$,

$$\hat{H}_0 = \sum_i |\Phi_i\rangle\langle\Phi_i|\hat{H}|\Phi_i\rangle\langle\Phi_i| = \sum_i H_{ii}|\Phi_i\rangle\langle\Phi_i|. \tag{2.54}$$

In this way, any state is an eigenstate of $\hat{H}_0$ with eigenvalue its energy. This is known as *Epstein-Nesbet (EN)* partitioning and leads to perturbation expansions in which the Δ denominators contain differences of diagonal matrix elements of the full Hamiltonian, i.e. $H_{ii} - H_{00}$. Unlike MP partitioning which deals with traces of matrices over hole states, the EN partitioning is *not* invariant under unitary transformation among particle and hole states.

2.7   Diagrammatic notation

To help generate and manipulate second-quantised expressions, in particular normal ordered ones, we will introduce diagrammatic notation. This section will only cover rules of interpretation for one-particle operators as found in [12, Ch. 4]. In quantum mechanics, there is a 'time sequence' to the application of operators (right-to-left). In diagrams this sequence is down-to-up

$$t \uparrow$$

Slater determinants

As previously mentioned, the reference state $|\Phi_0\rangle$ is the Fermi vacuum. It is represented by nothing:

$$\Phi_0 = \tag{2.55}$$

All other Slater determinants are represented by directed vertical or diagonal lines. *particles point upwards* and *holes point downwards*. For example

$$\Phi_i^a = \quad i\downarrow \quad \uparrow a \qquad \Phi_{ij}^{ab} = \quad i\downarrow\uparrow a \; j\downarrow\uparrow b \tag{2.56}$$

where bras and kets are specified by double lines above or below the diagram respectively. This is muted when taking the reference expectation value.

$$|\Phi_i^a\rangle = \{\hat{a}^\dagger\hat{i}\}|\Phi_0\rangle = \quad i\downarrow \quad \uparrow a \tag{2.57}$$

One-body operators

Take for example $\langle b|\hat{u}|a\rangle\{\hat{b}^{\dagger}\hat{a}\}$, we indicate with a marker (here a cross with dashes) the multiplicative factor $\langle b|\hat{u}|a\rangle$. The original ket $|\Phi_i^a\rangle$ becomes $|\Phi_i^b\rangle$ following the action of a normal ordered 1B operator $\hat{U}_{\mathrm{N}}$ at the vertex. The mnemonics OCB and IAK detail how to label the matrix elements with respect to hole/particle arrows.

$$(2.58)$$

In general we can represent normal ordered one-body operators as

$$\hat{U}_{\mathrm{N}} = \sum_{pq}\langle p|\hat{u}|q\rangle\{\hat{p}^{\dagger}\hat{q}\}$$

$$(2.59)$$

whereas the full operator must also include the 'bubble'

$$\hat{U} = \hat{U}_{\mathrm{N}} + \langle\Phi_0|\hat{U}|\Phi_0\rangle = \hat{U}_{\mathrm{N}} + \sum_{i} \text{} \quad i \quad . \tag{2.60}$$

A diagram in (2.59) is to be contracted in all valid ways in which states above and below interact. The only non-zero contractions $\overset{\frown}{\hat{i}^{\dagger}\hat{j}} = \delta_{ij}$ and $\overset{\frown}{\hat{a}\hat{b}^{\dagger}} = \delta_{ab}$ are represented as

$$(2.61)$$

To learn more about Hugenholtz diagrams and anti-symmetrised Goldstone diagrams see the rest of [12, Ch. 4].

③ IMSRG Formalism

To simplify *ab initio* many-body calculations, we want to decouple physics at different scales of energy by block-diagonalising the Hamiltonian with respect to a reference. The IMSRG formalism provides a way to systematically improve such techniques. This section is primarily taken from [16] and [15, Ch. 10].

3.1 Flow equation

Suppose we have a many-body system in some state $|\psi\rangle$, then the eigenvalue problem to find that system's spectrum is posed by the time-independent Schrödinger equation, omitting hats on operators

$$H|\psi\rangle = E|\psi\rangle. \tag{3.1}$$

We want to use a unitary similarity transformation (hence the name *similarity* renormalisation group) so that

$$H(s) \equiv U(s)H(0)U^\dagger(s), \tag{3.2}$$

which is parametrised by the *flow parameter s*. We choose a reference $|\Phi_0\rangle$ (see 2.2) which is our initial guess of the exact ground state energy eigenket. Alternatively, we could think of the exact states transforming as

$$|\psi\rangle \equiv \lim_{s\to\infty} U^\dagger(s)|\Phi_0\rangle, \tag{3.3}$$

analogously to the Schroödinger/Heisenberg pictures for time evolution of a quantum-mechanical system. We are transforming a non-vacuum, so a medium reference state (hence the name *in-medium* as opposed to in-vacuo). Consistency requires

$$U(0) = U^\dagger(0) = I, \qquad \langle\Phi_0|H(0)|\Phi_0\rangle = E_0, \tag{3.4}$$

$$\lim_{s\to\infty}\langle\Phi_0|H(s)|\Phi_0\rangle = \lim_{s\to\infty}\langle\Phi_0|U(s)H(0)U^\dagger(s)|\Phi_0\rangle = \langle\psi|H(0)|\psi\rangle = E. \tag{3.5}$$

We can freely impose the following condition on the unitary operator $U(s)$

$$\frac{d}{ds}U(s) \equiv \eta(s)U(s) \stackrel{\text{unitarity}}{\implies} \frac{d}{ds}U^\dagger(s) = -U^\dagger(s)\eta(s), \tag{3.6}$$

such that we obtain the SRG *flow equation* for the transformed Hamiltonian by the product rule

$$\frac{d}{ds}H(s) = [\eta(s), H(s)]. \tag{3.7}$$

We call $\eta(s)$ the *generator* of the flow since it determines the behaviour of $U(s)$ and thus of the transformation itself. We choose $\eta(s)$ so that

$$H(s) \equiv H^{\mathrm{d}}(s) + H^{\mathrm{od}}(s) \overset{s \to \infty}{\to} H^{\mathrm{d}}(s), \tag{3.8}$$

where $H^{\mathrm{d}}(s)$ is 'diagonal' in the *core*. Usually the core is the collection of states occupied in the reference but not always. We will call *excluded* the states which are excitations from the core. This is convenient, because it becomes easy to read off E via

$$\lim_{s \to \infty} \langle \Phi_0 | H(s) | \Phi_0 \rangle = \lim_{s \to \infty} \langle \Phi_0 | H^{\mathrm{d}}(s) | \Phi_0 \rangle = E. \tag{3.9}$$

When we say the Hamiltonian becomes diagonal in the state $|\Phi_0\rangle$, we mean for all non-trivial particle-hole pairs

$$\lim_{s \to \infty} \langle \Phi_0 | H(s) | \Phi_{ij\dots}^{ab\dots} \rangle \equiv 0. \tag{3.10}$$

If we think of a schematic, finite matrix representation of the Hamiltonians, this decoupling becomes clearer.
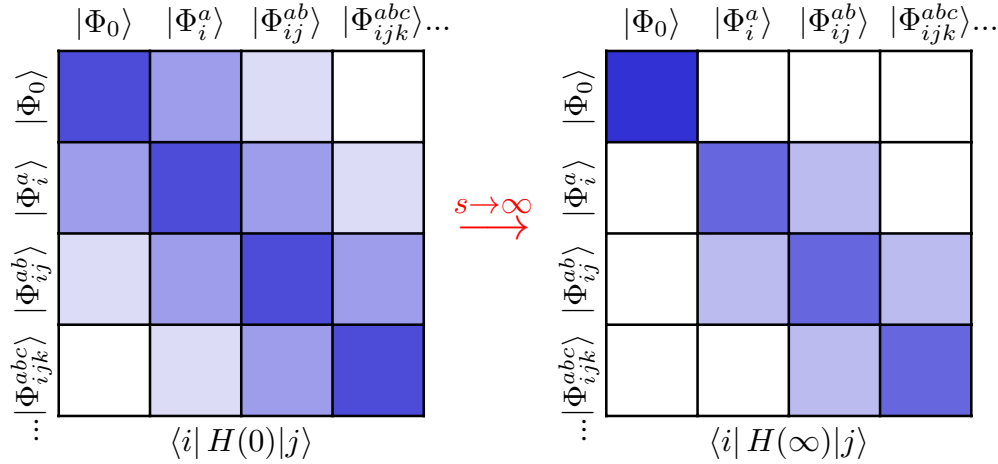
Fig. 6 As $s \to \infty$, the Hamiltonian becomes block-diagonal, i.e. the reference state decouples from any particle-hole excitation. There are no restrictions on the block connecting excitations.

If no reference state is given, convention tells us to use the true vacuum as the *free-space reference state*. The number after 'IMSRG' indicates the particle rank after which we truncate the induced normal ordered operators at each calculation. For example, when evaluating an operator commutator $[\hat{A}, \hat{B}] = \hat{C}$ or product $\hat{A}\hat{B} = \hat{C}$;

$$\hat{C} = \langle \Phi_0 | \hat{C} | \Phi_0 \rangle + \underbrace{\sum_{pq} X_{pq} \{\hat{p}^\dagger \hat{q}\} + \frac{1}{4} \sum_{pqrs} Y_{pqrs} \{\hat{p}^\dagger \hat{q}^\dagger \hat{s}\hat{r}\}}_{\text{IMSRG (2)}} + \frac{1}{36} \sum_{mnpqrs} Z_{mnpqrs} \{\hat{m}^\dagger \hat{n}^\dagger \hat{p}^\dagger \hat{s}\hat{r}\hat{q}\} + \dots \tag{3.11}$$

$$\underbrace{\phantom{\hat{C} = \langle \Phi_0 | \hat{C} | \Phi_0 \rangle + \sum_{pq} X_{pq} \{\hat{p}^\dagger \hat{q}\} + \frac{1}{4} \sum_{pqrs} Y_{pqrs} \{\hat{p}^\dagger \hat{q}^\dagger \hat{s}\hat{r}\} + \frac{1}{36} \sum_{mnpqrs} Z_{mnpqrs} \{\hat{m}^\dagger \hat{n}^\dagger \hat{p}^\dagger \hat{s}\hat{r}\hat{q}\}}}_{\text{IMSRG (3)}}$$

As seen in (2.33), a KB and LB operator commute to give a sum of MB operators

$$[K, L] \rightarrow M, \tag{3.12}$$

for $|K - L| \leq M \leq K + L - 1$. For a simple product of operators that range is $|K - L| \leq M \leq K + L$. If we sum over N states during the matrix multiplication, the product's spatial complexity would scale as N^{K+L+M}. For IMSRG (3) we have $M \leq 3$ so that $[2, 2] \rightarrow 3$, $[2, 3] \rightarrow 3$ and $[3, 3] \rightarrow 3$ are all possible commutator scenarios. We usually use shell model spinorbitals with $N \geq 20$ so the scalings N^7, N^8 and N^9 differ significantly [17].

To limit computational cost while maintaining the increased accuracy, we will also use IMSRG (3n7) which limits the surviving 3B operators of IMSRG (3) to commutator and product diagram topologies corresponding to $\mathcal{O}(N^7)$.

3.2 Magnus formulation

One choice of unitary transformation is defined by the *Magnus formulation* [18],

$$U(s) \equiv e^{\Omega(s)}. \tag{3.13}$$

Unitarity of $U(s)$ implies that the *Magnus operator* satisfies $\Omega^\dagger(s) = -\Omega(s)$. From (3.6), we get the 'flow equation' for $\Omega(s)$ [18]

$$\frac{d}{ds}\Omega(s) = \sum_{n=0}^{\infty} \frac{B_n}{n!} c_\Omega^n(\eta), \tag{3.14}$$

where B_n are the Bernoulli numbers and c_Ω^n are nested commutators

$$c_\Omega^0(\eta) \equiv \eta, \qquad c_\Omega^n(\eta) \equiv \left[\Omega, c_\Omega^{n-1}(\eta)\right]. \tag{3.15}$$

Operators evolve as $\hat{\mathcal{O}}(s) = e^{\Omega(s)}\hat{\mathcal{O}}(0)e^{\Omega(s)}$ where

$$\hat{\mathcal{O}}(s) = \hat{\mathcal{O}}(0) + \frac{1}{1!}\left[\Omega(s), \hat{\mathcal{O}}(0)\right] + \frac{1}{2!}\left[\Omega(s), \left[\Omega(s), \hat{\mathcal{O}}(0)\right]\right] + ... \tag{3.16}$$

We can numerically evolve $\Omega(s)$ using (3.14)and subsequently apply (3.16) to transform any operator along the IMSRG flow.

3.3 Choice of generator $\eta(s)$

Following [16], we saw in 3.1 that we want to decouple the reference by suppressing the offdiagonal part of the Hamiltonian, H^{od}. But we still have the freedom to chose $\eta(s)$ as long as it drives $H^{\mathrm{od}}(s) \rightarrow 0$ along the flow. Two appropriate generators for the single reference case are the White generator and the imaginary time generator.

White generator

We start by reminding ourselves of the definition of H^{od}. It connects the references to excitations and so has the form

$$H^{\text{od}} = \sum_{ai} f_{ai}\{\hat{a}^{\dagger}\hat{i}\} + \frac{1}{4}\sum_{abij}\Gamma_{abij}\{\hat{a}^{\dagger}\hat{b}^{\dagger}\hat{j}\hat{i}\} + \frac{1}{36}\sum_{abcijk} W_{abcijk}\{\hat{a}^{\dagger}\hat{b}^{\dagger}\hat{c}^{\dagger}\hat{k}\hat{j}\hat{i}\}. \tag{3.17}$$

The *White generator* is defined as

$$\eta(s) \equiv \frac{H^{\text{od}}(s)}{\Delta} \tag{3.18}$$

$$= \sum_{ai} \frac{f_{ai}}{\Delta_{ai}}\{\hat{a}^{\dagger}\hat{i}\} + \frac{1}{4}\sum_{abij}\frac{\Gamma_{abij}}{\Delta_{abij}}\{\hat{a}^{\dagger}\hat{b}^{\dagger}\hat{j}\hat{i}\} + \frac{1}{36}\sum_{abcijk}\frac{W_{abcijk}}{\Delta_{abcijk}}\{\hat{a}^{\dagger}\hat{b}^{\dagger}\hat{c}^{\dagger}\hat{k}\hat{j}\hat{i}\},$$

where we meet our old friend the energy denominator Δ (2.6). The operators f, Γ and W all flow with s and so does Δ. Up to particle rank of 2, with MP partitioning $\Delta_{ab...ij...}$ is defined as

$$\Delta_{ai} = f_{aa} - f_{ii} + \Gamma_{aiai}, \tag{3.19}$$

$$\Delta_{abij} = f_{aa} + f_{bb} + \Gamma_{abab} - f_{ii} - f_{jj} - \Gamma_{ijij} \tag{3.20}$$

$$- \Gamma_{aiai} - \Gamma_{bjbj} - \Gamma_{ajaj} - \Gamma_{bibi},$$

Using EN partitioning the denominator matrix elements are

$$\Delta_{ai} = \langle\Phi_i^a|H|\Phi_i^a\rangle - E_0 = \langle\Phi_0|\{\hat{i}^{\dagger}\hat{a}\}H\{\hat{a}^{\dagger}\hat{i}\}|\Phi_0\rangle - E_0, \tag{3.21}$$

$$\Delta_{abij} = \langle\Phi_{ij}^{ab}|H|\Phi_{ij}^{ab}\rangle - E_0 = \langle\Phi_0|\{\hat{i}^{\dagger}\hat{j}^{\dagger}\hat{a}\hat{b}\}H\{\hat{a}^{\dagger}\hat{b}^{\dagger}\hat{i}\hat{j}\}|\Phi_0\rangle - E_0. \tag{3.22}$$

Imaginary time generator

The *imaginary time (IT) generator* is instead defined as

$$\eta(s) \equiv \frac{H^{\text{od}}(s)}{\text{sgn}(\Delta)} \tag{3.23}$$

$$= \sum_{ai} \text{sgn}(\Delta_{ai})f_{ai}\{\hat{a}^{\dagger}\hat{i}\} + \frac{1}{4}\sum_{abij}\text{sgn}(\Delta_{abij})\Gamma_{abij}\{\hat{a}^{\dagger}\hat{b}^{\dagger}\hat{j}\hat{i}\} + \dots . \tag{3.24}$$

in terms of the sign of Δ;

$$\text{sgn}(\Delta) = \begin{cases} +1 & \Delta > 0, \\ -1 & \Delta < 0. \end{cases} \tag{3.25}$$

Here we note the sensitivity of the flow on energy level separation for both the White and IT generators. If the orbital energy spacings are not far enough, $\eta(s) \sim H^{od}$ will not be suppressed due to a small energy denominator Δ and the flow will *diverge* away from the targeted decoupling.

④ Spurious Isospin Symmetry Breaking

Since $\langle T^2 \rangle$ is misbehaved, by looking at Fig. 7, and $T^2 \sim (T^+T^- + T^-T^+)$ it was evident that the code at the start of the project could not accurately handle calculations regarding $\langle T^\pm \rangle$ and thus δ_C. Since δ_C is of the order 1%[1], we should try to have a firm understanding of all sources of isospin symmetry breaking in the IMSRG++[19], and try to control them. Throughout this section, we will seek to specifically understand sources of *spurious* ISB, which is just ISB arising even though it is not predicted (due to approximations in the Hamiltonian, for example).

4.1 Evidence for spurious ISB

As mentioned in section 0, we seek a framework with which to compute δ_C. In particular, it should reliably handle calculations involving $\langle T^2 \rangle$ and thus $\langle T^\pm \rangle$. This means that if there were no *a priori* sources of ISB, i.e. we introduce a nuclear potential faithful to the description of the shell model while including *no* Coulombic interaction and *no* pion-exchange mass or abundance difference, isospin symmetry should be observed.

A candidate for such a non-Coulombic attractive potential is the Minnesota potential, which is the sum of two inverted Gaussians. Looking at Fig. 7, S. Stroberg's IMSRG++ code for a ^{14}O post-Hartree-Fock Minnesota reference state found that, as the flow parameter tends to infinity, the isospin *does not* converge as expected. There are 8 protons and 6 neutrons in ^{14}O. The net isospin of the nucleus is $t = 1$ as seen in section 1.6. But the expectation value of T^2 did not converge to a perfect $\langle T^2 \rangle = t(t+1) = 2$ with the IMSRG flow. After extending the IMSRG truncation to IMSRG(3), the error ($\lim_{s \to \infty} \langle T^2(s) \rangle - 2$) actually grew instead of being reduced (see Fig. 8).
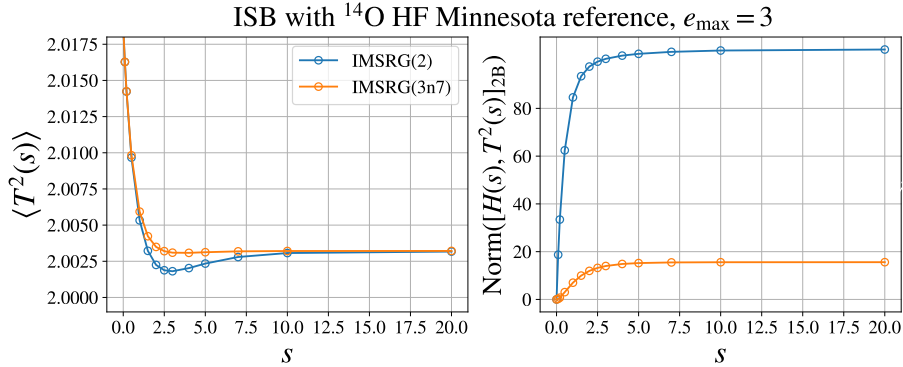
Fig. 7 Isospin symmetry is broken under S. Stroberg's IMSRG flow of ^{14}O HF Minnesota potential reference state. (Left) The isospin $\langle T^2(s) \rangle$ should trend to 2 as $s \to \infty$ and (Right) the two-body part of the commutator $[H(s), T^2(s)]$ should be identically 0 if T^2 is conserved. Presented at [20], reproduced here.

4.2   Sources of spurious ISB

Fig. 7 had numerical parameters `hw=16` (MeV) and `cLS=-5.00`. From now on we will set `hw=25`, `cLS=-10.00` to prevent the inversion of energy levels in our toy model. Going back to 1.3, we can express the reference as a linear combination of harmonic oscillator eigenstates with quantum number N. Because it's impossible to store infinitely many states on a computer, we truncate the basis at $N = 2n + \ell \leq e_{\max}$. In parallel to my work, Jonathan Riess investigated the $e_{\max}$ truncation's contribution to the ISB. He found that it did not account for most of the error. (This truncation was not expected to break isospin since it does not discriminate between p^+ and n^0 energy levels.) Continuing with the same ^{14}O reference, after finding that the error did not significantly depend on the energy level spacing $\hbar\omega$ either, the importance of orbital population was investigated. It was found that for certain orbital spaces, i.e. depending on which shells are included in the model space of the nucleus, there was a much greater lack of convergence to 2 (Fig. 8). At the IMSRG(2) approximation, when the model space was reduced to the $0p_{3/2}$, $0p_{1/2}$ and $0d_{5/2}$ energy shells, the error was acute relative to the full $e_{\max} = 3$ model space for ^{14}O.
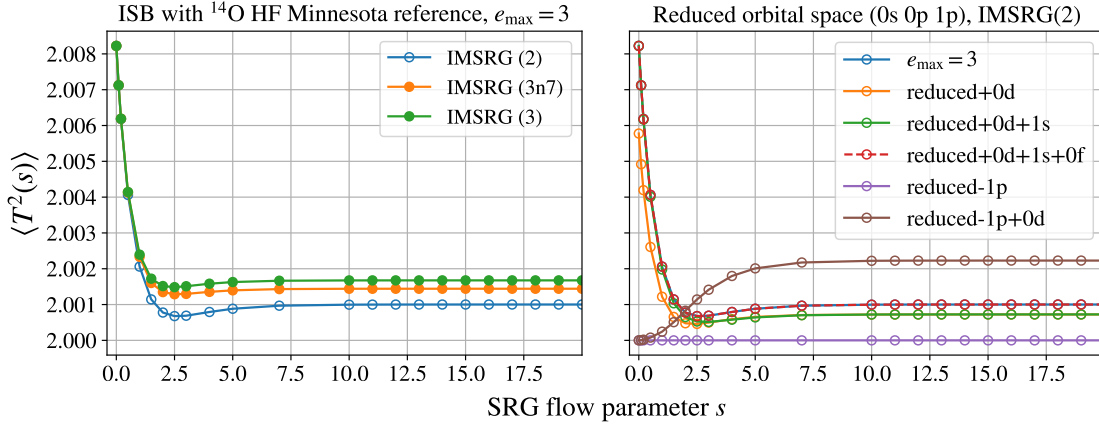

Fig. 8 (Left) IMSRG truncation is relaxed yet the error in $\langle T^2(\infty)\rangle$ does not decrease. (Right) Different orbital spaces display different convergence behaviours.

The Hartree Fock diagonalisation step (2.40) is responsible for the ISB at $s = 0$. This is because we express T^2 as normal ordered with respect to a HF eigenstate, for which protons and neutrons see a different mean field since there are more protons than neutrons in the reference. Because of the overlap integrals in (2.42), this immediate ISB only occurs when $N \neq Z$ and there are orbitals with same ℓ but different n quantum numbers [4].

Hoping to track what caused the error in the unrestricted case, an investigation into the source of error in the $0p_{3/2}$, $0p_{1/2}$, $0d_{5/2}$ model space was warranted. To pinpoint the source of error even further, the cumulative sum (3.16) in the Magnus evolution of $\langle T^2 \rangle$ was evaluated term by term as in Fig. 9. It indicated that the source of isospin symmetry breaking was the third term in (3.16); the nested commutator

$$\langle \left[\Omega(s), \left[\Omega(s), T^2(0)\right]\right]\rangle. \tag{4.1}$$

---

[4]For ^{14}O reduced orbitals in Fig. 8 there are several 'echelons' of HF mixing; none, including just 1s *or* 1p and including both 1s *and* 1p. ISB in configurations with initial HF mixing may be fixed by adding correlations with IMSRG flow as with the 0d and 0d+1s cases.
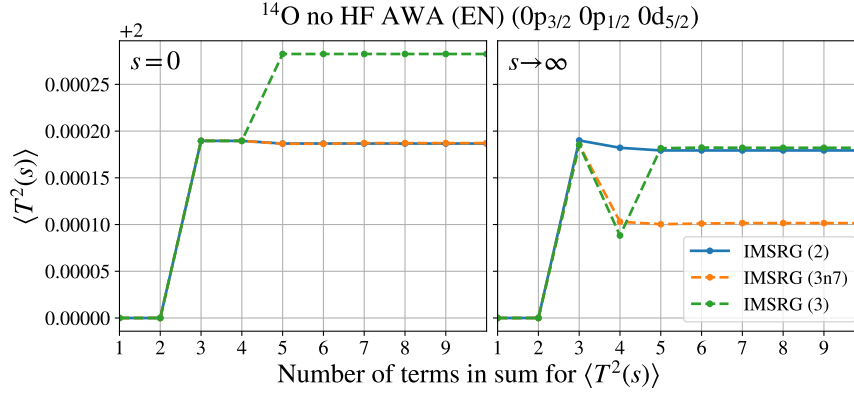
Fig. 9 (Left) Cumulative sum shows that the third term in (3.16) is problematic for an asymmetric ^{14}O reference and offdiagonal to be decoupled using the White generator with Epstein-Nesbet partitioning.

(Right) When $\Omega(s) \approx \eta(s)$ is evolved as $s \to \infty$, the third term persists.

But we were using the White generator (see 3.3),

$$\eta(s) \equiv \frac{H^{\mathrm{od}}}{\Delta} \implies \lim_{s \to \infty} \eta(s) = 0. \tag{4.2}$$

Looking at (3.14) with η small, we make the approximation $\Omega \approx \eta$ and expand (4.1) explicitly

$$\left\langle \left[\eta(s), \left[\eta(s), T^2(0) \right] \right] \right\rangle = \langle \Phi_0 | (\eta^2(s) T^2(0) - 2\eta(s) T^2(0) \eta(s) + T^2(0) \eta^2(s)) | \Phi_0 \rangle, \tag{4.3}$$

where $|\Phi_0\rangle$ is the ^{14}O HF Minnesota reference state. We will now evaluate this commutator analytically using Hugenholtz and ASG diagrams [12] in order to further understand why this commutator did not vanish.

Recall the rules for commutators of normal ordered operators (2.33). Setting the 1B and 3B parts of Ω to zero did not affect the code's evaluation of (4.1), while erasing the 2B part eliminated it. This meant we should only consider products in the commutator which yield a non-zero 0B and involve the 2B part of Ω, which we call $\Omega_{2\mathrm{B}}$. Since the outer commutator in (4.3) must be between $\eta_{2\mathrm{B}}$ and the inner commutator, we need only consider the parts of T^2 which give a non-zero $\left[\eta_{2\mathrm{B}}, T^2 \right]_{2\mathrm{B}}$ since we are looking for an overall 0B term. This leaves only $T^2_{1\mathrm{B}}$ and T^2_{2B}. Because H^{od} only connects the reference state with excited states, so does $\eta_{2\mathrm{B}}$. This means the only two-body diagrams $\eta_{2\mathrm{B}}$ can produce are

and .
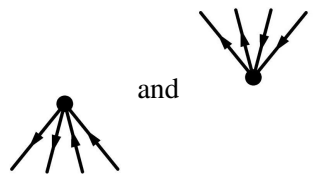
As a result, both the $\eta^2 T^2$ and $T^2 \eta^2$ terms from the commutator can't be fully contracted down to a 0B term given T_{1B}^2 or T_{2B}^2 at either end of the diagram. Equation (4.1) reduces down to

$$\langle [\Omega(s), [\Omega(s), T^2(0)]] \rangle = -2\langle \Phi_0 | \eta(s) T^2(0) \eta(s) | \Phi_0 \rangle$$
$$= -2\langle \Phi_0 | \eta_{2B}(s) T_{1B}^2(0) \eta_{2B}(s) | \Phi_0 \rangle - 2\langle \Phi_0 | \eta_{2B}(s) T_{2B}^2(0) \eta_{2B}(s) | \Phi_0 \rangle. \tag{4.4}$$

These terms correspond to the two Hugenholtz skeletons in Fig. 10, and can now be evaluated. To save space, we will write the anti-symmetrised two-body (2B) matrix elements as

$$\eta_{pqrs} = \langle pq | \eta | rs \rangle - \langle pq | \eta | sr \rangle,$$

and similarly for T_{pqrs}^2. The matrix elements of the 1B and anti-symmetrised 2B parts of normal ordered T^2 are found starting with (1.25), where $\overline{\mu}$ is the orbital μ with t_z flipped.

$$T_{pq}^2 = \frac{3}{4}\delta_{pq} + \sum_k n_k T_{pkqk}^2,$$

$$T_{pqrs}^2 = \begin{cases} C_{\text{noflip}}(\delta_{pr}\delta_{qs} - \delta_{ps}\delta_{qr}) & \text{nucleon type is not changed,} \\ C_{\text{flip}}(\delta_{p\bar{r}}\delta_{q\bar{s}} - \delta_{p\bar{s}}\delta_{q\bar{r}}) & \text{p}^+ \text{ goes to n}^0 \text{, vice versa.} \end{cases}$$

$C_{\text{noflip}} = 1/2$ and $C_{\text{flip}} = 1$ as in (1.25) but we can keep them explicit to track the influence of each part of T_{pqrs}^2.
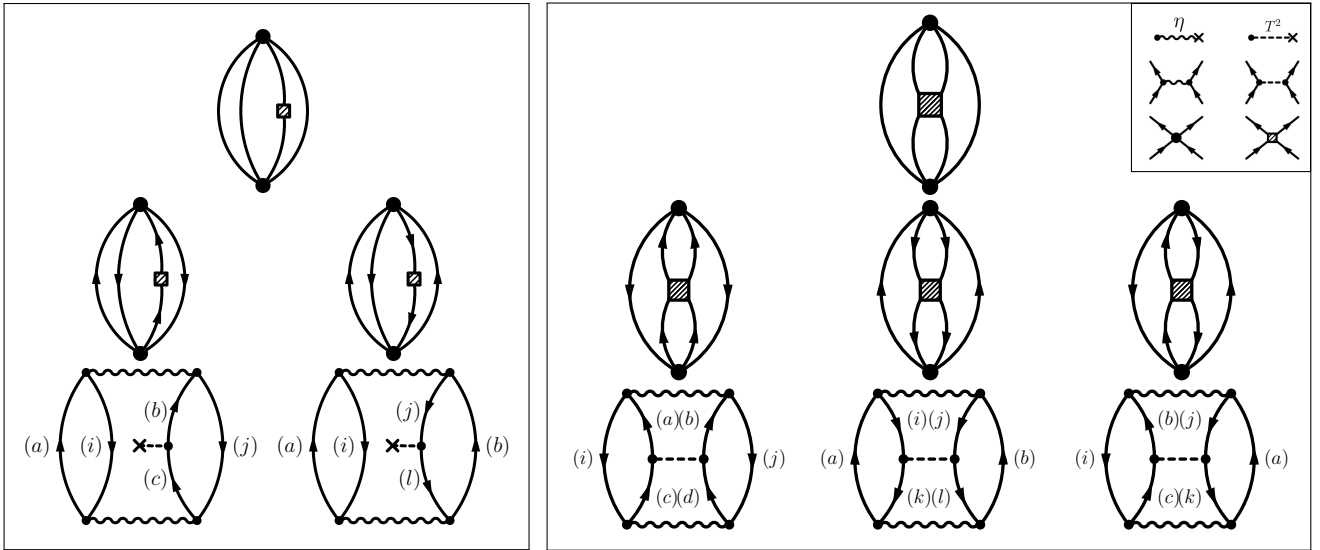
Fig. 10 Diagrammatic notation for the T_{1B}^2 term (left) and T_{2B}^2 term (right) in (4.4). Hugenholtz skeletons are expanded into directed Hugenholtz diagrams each of which are then expanded into anti-symmetrised Goldstone diagrams (ASG). These can finally be interpreted according to rules laid out in [12].

Adding all 5 ASG diagrams yields (see appendix)

$$\langle[\eta(s),[\eta(s),T^2(0)]]\rangle = -2\sum_{abij}\Big[\eta_{ijab}\big(\overbrace{\tfrac{1}{2}\eta_{abij}(n_{\bar{j}}-n_{\bar{b}})}^{T^2_{1B}}+\overbrace{\tfrac{1}{4}\eta_{\bar{a}\bar{b}ij}\bar{n}_{\bar{a}}\bar{n}_{\bar{b}}}^{T^2_{2B}\text{ p ladder}}+\overbrace{\tfrac{1}{4}\eta_{ab\bar{i}\bar{j}}n_{\bar{i}}n_{\bar{j}}}^{T^2_{2B}\text{ h ladder}}-\eta_{a\bar{b}i\bar{j}}\bar{n}_{\bar{b}}n_{\bar{j}}\big)+\overbrace{\eta_{ij\bar{a}\bar{j}}\eta_{ab\bar{i}b}\bar{n}_{\bar{j}}n_{\bar{b}}}^{T^2_{2B}\text{ ring}}\Big].$$

$$(4.5)$$

The above expression only comes from the isospin-flipping matrix elements of T^2, since $[\eta(s),T^z(0)] = 0$. The absence of any C_{noflip} factor in the final expression in the appendix agrees with this expectation. (4.5) was found to agree with IMSRG++ for every attempted configuration of the model space.

Asymmetric $|\Phi\rangle$

In our notation, where $a, b, c, ...$ refer to particle states and $i, j, k, ...$ refer to hole states, the occupation numbers n_j and $\bar{n}_b$ are redundant, as these spinorbitals are *necessarily* filled and empty respectively. However, the occupation number $n_{\bar{b}}$ and hole number $\bar{n}_{\bar{j}}$ only necessarily vanish for a symmetric reference, for which j and $\bar{j}$ are both hole states and b and $\bar{b}$ are both particle states ($N = Z$). For the RHS of (4.5) to vanish, we should then have a symmetric reference *and* $\eta_{2B}(s)$ as we will see.

Asymmetric $\eta(s)$

For a symmetric reference, if $\eta_{abij} = \eta_{\bar{a}\bar{b}ij} = \eta_{\bar{a}b\bar{i}j} = \eta_{\bar{a}bi\bar{i}} = ...$, then the sum trivially vanishes. Note we must have an even number of overlined indices to respect charge conservation. Since $\eta_{abij}(s) = H^{\text{od}}_{abij}/\Delta_{abij}$, there are two contributors to the isospin asymmetry;

- $H^{\text{od}}_{abij} = \tfrac{1}{4}\Gamma_{abij}\{\hat{a}^\dagger\hat{b}^\dagger\hat{j}\hat{i}\}$ (3.17) spoils isospin symmetry for an asymmetric core and thus excitations,

- $\Delta_{abij}\begin{cases}\text{Møller-Plesset} & (3.20)\\ \text{Epstein-Nesbet} & (3.22)\end{cases}$ matrix elements break symmetry for asymmetric reference.

If η_{2B} is not isospin-symmetric, (4.5) does not necessarily vanish as desired. If on top of this the reference is also asymmetric, this could add another source of ISB due to $n_{\bar{b}}$ and $\bar{n}_{\bar{j}}$.

Config.	$|\Phi_0\rangle$	S	S	S	S	A	A	A	A
	$\eta(s)$	W	W	IT	IT	W	W	IT	IT
	H^{od}	S	A	S	A	S	A	S	A
Epst-Nesb		0.001868	0.098568	0.000000	76.906202	0.000379	0.000379	0.000000	0.000000
Møll-Pless		0.000000	0.303273			0.000833	0.000833		
HF Ep-Ne		0.00123	0.093808	0.000000	214.325843	0.000142	0.004746	0.318964	14.650016
HF Mø-Pl		0.000000	0.212356			0.000271	0.006557		

Table 1 $\langle[\eta(s),[\eta(s),T^2(0)]]\rangle$ at IMSRG(2) $s = 0$ for different configurations with the ^{14}O (or ^{16}O) reduced orbital space $0p_{3/2}$, $0p_{1/2}$ and $0d_{5/2}$ with and without the HF diagonalisation step and 1p orbitals. See Fig. 11.

We can compare these considerations to a numerical calculation of the second nested commutator. In Table 1, the symmetric (S) reference option is ^{16}O ($N = Z$) while the asymmetric (A) one is good old ^{14}O (see Fig. 11). The White generator and imaginary time generators are abbreviated as W and IT respectively. A symmetric offdiagonal H^{od} definition entails that we welcome the unoccupied neutron $0p_{1/2}$ orbital as part of the core to be decoupled, while the asymmetric definition excludes it. Møller-Plesset and Epstein-Nesbet partitionings of Δ for the White
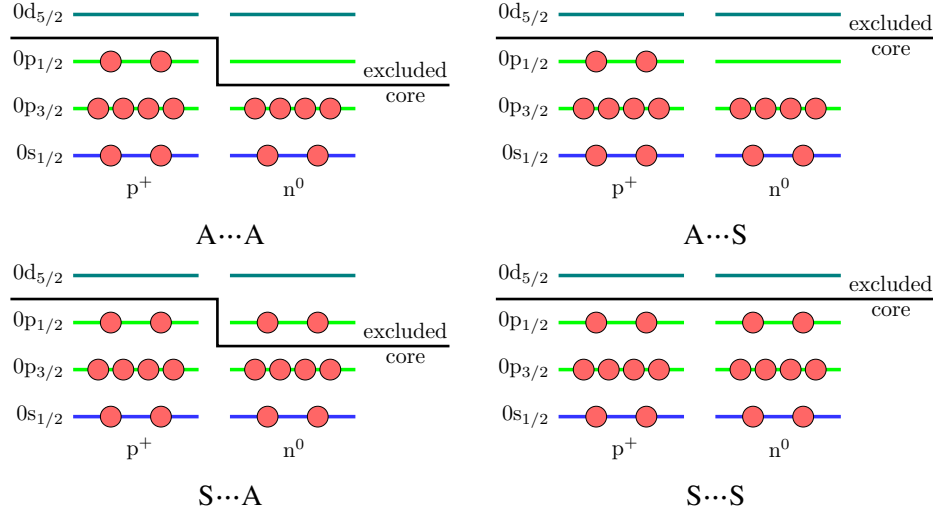
Fig. 11 The different configurations of the reduced orbital space based on the isospin symmetry of the reference and H^{od} respectively. For example, A···S is a model space with asymmmetric (A) reference but symmetric (S) offdiagonal definition.

generator $\eta(s) = H^{od}/\Delta$ both lead to spurious ISB. However, for the MP case of SWS, the commutator vanished. This is because neither the reference (and thus Δ) nor H^{od} broke isospin symmetry.

When the imaginary generator was substituted, the error vanished for a symmetric reference and H^{od} (and thus η). This is because, as in the SWS MP case, the denominator did not asymmetrise η despite H^{od} being symmetric.

From Table 1, we see the IT generator does not discriminate between EN and MP partitioning. This is because we construct the model space such that the energy levels are non-degenerate enough to allow $\lim_{s\to\infty} \eta(s) = \lim_{s\to\infty} H^{od}/\Delta = 0$, which means Δ is sufficiently big to ensure there is no risk of different partitioning leading to different $\text{sgn}(\Delta)$.

Importantly, $\langle T^2 \rangle$ should exactly be equal to 2 for ^{14}O or 0 for ^{16}O since we have removed authentic sources of ISB. Either way, the second nested commutator contributed more error than any other term, so should be eliminated.

The sum (4.5) was reindexed in terms of orbital quantum numbers and isospin-basis elements for a symmetric reference, e.g. in terms of $\langle T = 1, T^z = 1|\eta|T = 1, T^z = 1\rangle$,..., and was found to agree with the computed commutator (see appendix). Looking at Table 1, the HF diagonalisation step seems to introduce spurious ISB before IMSRG. After exploration, this ISB persists after IMSRG flow which should be investigated.

4.3   Remedies for spurious ISB

Eliminating the problematic commutator (4.1) by switching to an isospin-symmetric energy denominator remedied the spurious ISB caused by $\eta(s)$ for isospin-symmetric $|\Phi_0\rangle$ and H^{od}. This is shown in Fig. 12 and Fig. 13 below. If the calculation demanded an asymmetric reference, then at some of the highlighted terms in (4.5) sum might
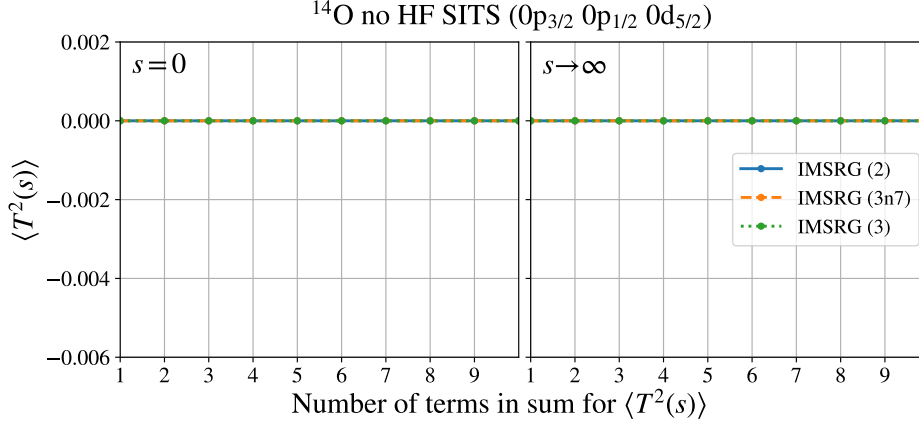
Fig. 12 (Left) For a symmetric offdiagonal, the imaginary time generator as a whole is isospin symmetric. So when we consider a symmetric reference, the sum (4.5) vanishes. The rest of the nested commutators are muted by the factorial in the denominator (see (3.16)).
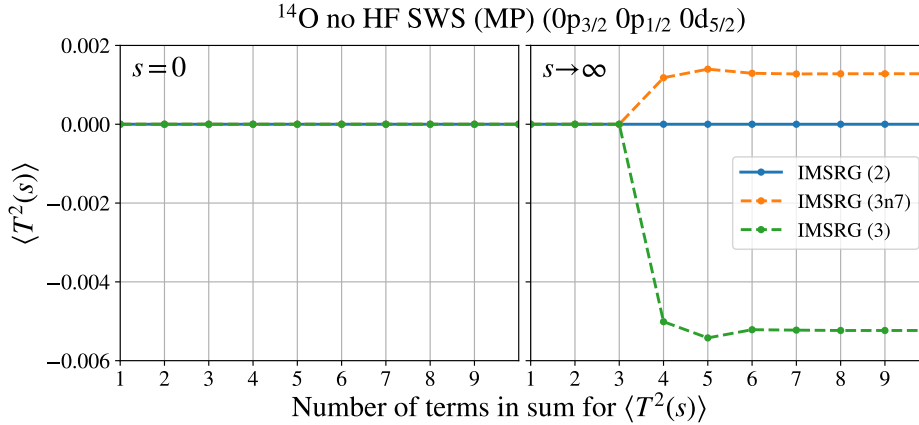
Fig. 13 (Left) MP partitioning of Δ paired with an isospin-symmetric H^{od} render the White generator $\eta(s)$ isospin-symmetric. As in Fig. 12, the sum vanishes for a symmetric reference as a result.

not vanish. But those without $n_{\bar{b}}$ or $\bar{n}_{\bar{j}}$ would cancel for a symmetric generator $\eta(s)$. This is apparent in Table 1 when going from AWS to AITS, whereby the generator becomes symmetric so that the term vanishes. In other words, symmetrising the generator reduces the spurious ISB but in principle it cannot be completely eliminated for an asymmetric reference IMSRG++ calculation.

⑤ Conclusion

After reviewing the basics of nuclear structure, redefining the many-body problem with the particle-hole formulation and introducing the IMSRG, we were able to identify three sources of spurious ISB in the IMSRG:

1. an asymmetric reference state $|\Phi_0\rangle$,

as well as an asymmetric energy denominator SRG flow generator $\eta(s)$, e.g. the White or imaginary time generator,

2. via an asymmetric energy denominator Δ,

3. via an isospin-asymmetric definition of H^{od} .

These sources were made manifest by analytically reducing the second nested commutator in the Magnus cumulative sum for $T^2(s)$ by employing diagrammatic notation and looking at particle and hole states.

We found that to remedy the spurious ISB caused by $\eta(s)$ in this commutator (which would greatly reduce the overall ISB), one would need to symmetrise Δ (by using the imaginary-time generator or employing MP partitioning for the White generator) and have a symmetric reference and offdiagonal definition.

This work lays a path forward for assessing spurious isospin symmetry breaking in $0^+ \rightarrow 0^+$ superallowed beta decays when $N \approx Z$. For such systems the spurious ISB caused by IMSRG++ can be greatly reduced by using a symmetric generator, which allows for more accurate calculations involving isospin. As we saw in the introduction, this is a step toward a reliable framework for calculating δ_{C}.

When diagonalising to the Hartree-Fock basis, the problematic commutator displayed curious behaviour as the IMSRG flowed, which needs to be better understood since realistic calculations usually involve a HF basis. The benefit of using a symmetric generator such as the imaginary-time generator should be investigated, in particular for neutrinoless double-beta decay where N and Z differ greatly [21].
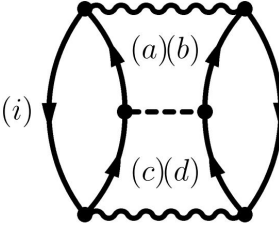
Appendix

T^2_{1B} diagrams

$$(a)\ \ (i)\ \times\text{-}\text{-}\bullet\ (j)\ +\ (a)\ \ (i)\ \times\text{-}\text{-}\bullet\ (b) = \frac{1}{2}\sum_{abcij}\eta_{ijab}T^2_{bc}\eta_{acij} - \frac{1}{2}\sum_{abijl}\eta_{ijab}T^2_{lj}\eta_{abil}$$

$$= \frac{1}{2}\sum_{abcij}\eta_{ijab}\Big(\frac{3}{4}\delta_{bc} + \sum_k T^2_{bkck}\Big)\eta_{acij} - \frac{1}{2}\sum_{abijl}\eta_{ijab}\Big(\frac{3}{4}\delta_{lj} + \sum_k T^2_{lkjk}\Big)\eta_{abil}$$

$$= \frac{3}{8}\sum_{abij}\eta_{ijab}(\eta_{abij} - \eta_{abij}) + \frac{1}{2}\sum_{abcijk}\eta_{ijab}T^2_{bkck}\eta_{acij} - \frac{1}{2}\sum_{abijkl}\eta_{ijab}T^2_{lkjk}\eta_{abil}$$

$$= \frac{1}{2}\sum_{abcijk}\eta_{ijab}\eta_{acij}\begin{cases}+C_{\text{noflip}}(\delta_{bc}\delta_{kk} - \delta_{bk}\delta_{kc})\\ +C_{\text{flip}}(\delta_{b\bar{c}}\delta_{k\bar{k}} - \delta_{b\bar{k}}\delta_{k\bar{c}})\end{cases} - \frac{1}{2}\sum_{abijkl}\eta_{ijab}\eta_{abil}\begin{cases}+C_{\text{noflip}}(\delta_{lj}\delta_{kk} - \delta_{lk}\delta_{kj})\\ +C_{\text{flip}}(\delta_{l\bar{j}}\delta_{k\bar{k}} - \delta_{l\bar{k}}\delta_{k\bar{j}})\end{cases}$$

$$\overset{\dagger}{=} \frac{1}{2}\sum_{abcijk}\eta_{ijab}\eta_{acij}\begin{cases}+C_{\text{noflip}}\delta_{bc}\delta_{kk}\\ -C_{\text{flip}}n_{\bar{b}}\delta_{b\bar{k}}\delta_{k\bar{c}}\end{cases} - \frac{1}{2}\sum_{abijkl}\eta_{ijab}\eta_{abil}\begin{cases}+C_{\text{noflip}}\delta_{lj}\delta_{kk} - C_{\text{noflip}}\delta_{lk}\delta_{kj}\\ -C_{\text{flip}}n_{\bar{j}}\delta_{l\bar{k}}\delta_{k\bar{j}}\end{cases}$$

$$= \frac{1}{2}\sum_{abcij}\eta_{ijab}\eta_{acij}\Big(C_{\text{noflip}}\delta_{bc}\sum_k\delta_{kk} - C_{\text{flip}}n_{\bar{b}}\sum_k\delta_{b\bar{k}}\delta_{k\bar{c}}\Big)$$

$$\quad - \frac{1}{2}\sum_{abijl}\eta_{ijab}\eta_{abil}\Big(C_{\text{noflip}}\delta_{lj}\sum_k\delta_{kk} - C_{\text{noflip}}\sum_k\delta_{lk}\delta_{kj} - C_{\text{flip}}n_{\bar{j}}\sum_k\delta_{l\bar{k}}\delta_{k\bar{j}}\Big)$$

$$\overset{\ddagger}{=} \frac{1}{2}C_{\text{noflip}}\sum_{abij}\eta_{ijab}\eta_{abij}\sum_k\delta_{kk} - \frac{1}{2}C_{\text{flip}}\sum_{abcij}n_{\bar{b}}\eta_{ijab}\eta_{acij}\delta_{bc}$$

$$\quad - \frac{1}{2}C_{\text{noflip}}\sum_{abij}\eta_{ijab}\eta_{abij}\sum_k\delta_{kk} + \frac{1}{2}C_{\text{noflip}}\sum_{abijl}\eta_{ijab}\eta_{abil}\delta_{lj} + \frac{1}{2}C_{\text{flip}}\sum_{abijl}n_{\bar{j}}\eta_{ijab}\eta_{abil}\delta_{lj}$$

$$= 0 - \frac{1}{2}C_{\text{flip}}\sum_{abij}n_{\bar{b}}\eta_{ijab}\eta_{abij} + \frac{1}{2}C_{\text{noflip}}\sum_{abij}\eta_{ijab}\eta_{abij} + \frac{1}{2}C_{\text{flip}}n_{\bar{j}}\sum_{abij}\eta_{ijab}\eta_{abij}$$

$$= \frac{1}{2}\sum_{abij}\eta_{ijab}\eta_{abij}(C_{\text{noflip}} + C_{\text{flip}}(n_{\bar{j}} - n_{\bar{b}}))$$

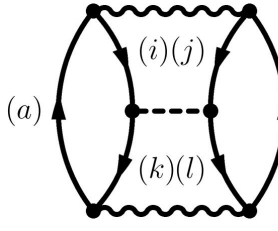$\dagger\,\delta_{ai} = 0$ since particle states cannot be hole states and $\delta_{a\bar{a}} = 0$.

$\ddagger\,\sum_k\delta_{l\bar{k}}\delta_{k\bar{j}} = \sum_k\delta_{l\bar{k}}\delta_{j\bar{k}} = \delta_{lj}.$

T_{2B}^2 particle ladder

$$
(i)\ \ \\ \ (j) = \frac{1}{8}\sum_{abcdij}\eta_{ijab}T^2_{abcd}\eta_{cdij} = \frac{1}{8}\sum_{abcdij}\eta_{ijab}\eta_{cdij}\begin{cases}+C_{\text{noflip}}(\delta_{ac}\delta_{bd}-\delta_{ad}\delta_{bc})\\+C_{\text{flip}}\bar{n}_{\bar a}\bar{n}_{\bar b}(\delta_{a\bar c}\delta_{b\bar d}-\delta_{a\bar d}\delta_{b\bar c})\end{cases}
$$

$$
= \frac{1}{8}\sum_{abcdij}\eta_{ijab}\eta_{cdij}\big(C_{\text{noflip}}(\delta_{ac}\delta_{bd}-\delta_{ad}\delta_{bc})+C_{\text{flip}}\bar{n}_{\bar a}\bar{n}_{\bar b}(\delta_{a\bar c}\delta_{b\bar d}-\delta_{a\bar d}\delta_{b\bar c})\big)
$$

$$
= \frac{1}{8}\sum_{abcdij}\eta_{ijab}\eta_{cdij}C_{\text{noflip}}(\delta_{ac}\delta_{bd}-\delta_{ad}\delta_{bc})+\frac{1}{8}\sum_{abcdij}\eta_{ijab}\eta_{cdij}C_{\text{flip}}\bar{n}_{\bar a}\bar{n}_{\bar b}(\delta_{a\bar c}\delta_{b\bar d}-\delta_{a\bar d}\delta_{b\bar c})
$$

$$
= \frac{1}{8}C_{\text{noflip}}\sum_{abij}\eta_{ijab}(\eta_{abij}-\eta_{baij})+\frac{1}{8}C_{\text{flip}}\sum_{abij}\bar{n}_{\bar a}\bar{n}_{\bar b}\eta_{ijab}(\eta_{\bar a\bar b ij}-\eta_{\bar b\bar a ij})
$$

$$
\overset{\dagger}{=} \frac{1}{4}C_{\text{noflip}}\sum_{abij}\eta_{ijab}\eta_{abij}+\frac{1}{4}C_{\text{flip}}\sum_{abij}\bar{n}_{\bar a}\bar{n}_{\bar b}\eta_{ijab}\eta_{\bar a\bar b ij}
$$

T_{2B}^2 hole ladder
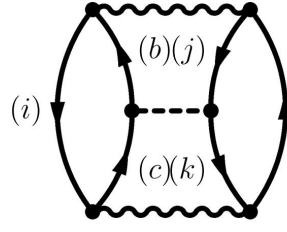
$$
(a)\ \ \\ \ (b) = \frac{1}{8}\sum_{abijkl}\eta_{ijab}T^2_{klij}\eta_{abkl} = \frac{1}{8}\sum_{abijkl}\eta_{ijab}\eta_{abkl}\begin{cases}+C_{\text{noflip}}(\delta_{ki}\delta_{lj}-\delta_{kj}\delta_{li})\\+C_{\text{flip}}n_{\bar i}n_{\bar j}(\delta_{k\bar i}\delta_{l\bar j}-\delta_{k\bar j}\delta_{l\bar i})\end{cases}
$$

$$
= \frac{1}{8}\sum_{abijkl}\eta_{ijab}\eta_{abkl}\big(C_{\text{noflip}}(\delta_{ki}\delta_{lj}-\delta_{kj}\delta_{li})+C_{\text{flip}}n_{\bar i}n_{\bar j}(\delta_{k\bar i}\delta_{l\bar j}-\delta_{k\bar j}\delta_{l\bar i})\big)
$$

$$
= \frac{1}{8}\sum_{abijkl}\eta_{ijab}\eta_{abkl}C_{\text{noflip}}(\delta_{ki}\delta_{lj}-\delta_{kj}\delta_{li})+\frac{1}{8}\sum_{abijkl}\eta_{ijab}\eta_{abkl}C_{\text{flip}}n_{\bar i}n_{\bar j}(\delta_{k\bar i}\delta_{l\bar j}-\delta_{k\bar j}\delta_{l\bar i})
$$

$$
= \frac{1}{8}C_{\text{noflip}}\sum_{abij}\eta_{ijab}(\eta_{abij}-\eta_{abji})+\frac{1}{8}C_{\text{flip}}\sum_{abij}n_{\bar i}n_{\bar j}\eta_{ijab}(\eta_{ab\bar i\bar j}-\eta_{ab\bar j\bar i})
$$

$$
\overset{\dagger}{=} \frac{1}{4}C_{\text{noflip}}\sum_{abij}\eta_{ijab}\eta_{abij}+\frac{1}{4}C_{\text{flip}}\sum_{abij}n_{\bar i}n_{\bar j}\eta_{ijab}\eta_{ab\bar i\bar j}
$$

[†]Terms double since antisymmetrised matrix elements satisfy $A_{pqrs}=-A_{qprs}$.

$T_{\mathbf{2B}}^2$ ring

$$(a) = -\sum_{abcijk} \eta_{ijba} T_{bkcj}^2 \eta_{caik} = -\sum_{abcijk} \eta_{ijba}\eta_{caik} \begin{cases} +C_{\text{noflip}}(\delta_{bc}\delta_{kj} - \delta_{bj}\delta_{kc}) \\ +C_{\text{flip}}(\bar{n}_{\bar{b}}n_{\bar{j}}\delta_{b\bar{c}}\delta_{k\bar{j}} - \bar{n}_{\bar{j}}n_{\bar{c}}\delta_{b\bar{j}}\delta_{k\bar{c}}) \end{cases}$$

$$= -\sum_{abcijk} \eta_{ijba}\eta_{caik} \begin{cases} +C_{\text{noflip}}\delta_{bc}\delta_{kj} \\ +C_{\text{flip}}\bar{n}_{\bar{b}}n_{\bar{j}}\delta_{b\bar{c}}\delta_{k\bar{j}} - C_{\text{flip}}\bar{n}_{\bar{j}}n_{\bar{c}}\delta_{b\bar{j}}\delta_{k\bar{c}} \end{cases}$$

$$= -C_{\text{noflip}}\sum_{abcijk} \eta_{ijba}\eta_{caik}\delta_{bc}\delta_{kj} - C_{\text{flip}}\sum_{abcijk} \eta_{ijba}\eta_{caik}\bar{n}_{\bar{b}}n_{\bar{j}}\delta_{b\bar{c}}\delta_{k\bar{j}} + C_{\text{flip}}\sum_{abcijk} \eta_{ijba}\eta_{caik}\bar{n}_{\bar{j}}n_{\bar{c}}\delta_{b\bar{j}}\delta_{k\bar{c}}$$

$$= -C_{\text{noflip}}\sum_{abij} \eta_{ijba}\eta_{baij} - C_{\text{flip}}\sum_{abij} \bar{n}_{\bar{b}}n_{\bar{j}}\eta_{ijba}\eta_{\bar{b}ai\bar{j}} + C_{\text{flip}}\sum_{acij} \bar{n}_{\bar{j}}n_{\bar{c}}\eta_{ij\bar{j}a}\eta_{cai\bar{c}}$$

$$= -\sum_{abij} \eta_{ijab}\left(C_{\text{noflip}}\eta_{abij} + C_{\text{flip}}\bar{n}_{\bar{b}}n_{\bar{j}}\eta_{ab\bar{i}\bar{j}}\right) + C_{\text{flip}}\sum_{abij} \bar{n}_{\bar{j}}n_{\bar{b}}\eta_{ijaj}\eta_{abi\bar{b}}$$

Reduced diagram sum

$$\langle[\eta(s),[\eta(s),T^2(0)]]\rangle = -2C_{\text{flip}}\sum_{abij}\Bigg[\eta_{ijab}\big(\overbrace{\tfrac{1}{2}\eta_{abij}(n_{\bar{j}}-n_{\bar{b}})}^{T_{1B}^2} + \overbrace{\tfrac{1}{4}\eta_{\bar{a}\bar{b}ij}\bar{n}_{\bar{a}}\bar{n}_{\bar{b}}}^{T_{2B}^2 \text{ p ladder}} + \overbrace{\tfrac{1}{4}\eta_{ab\bar{i}\bar{j}}n_{\bar{i}}n_{\bar{j}}}^{T_{2B}^2 \text{ h ladder}} - \eta_{ab\bar{i}\bar{j}}\bar{n}_{\bar{b}}n_{\bar{j}}\big) + \overbrace{\eta_{ijaj}\eta_{abib}\bar{n}_{\bar{j}}n_{\bar{b}}}^{T_{2B}^2 \text{ ring}}\Bigg]$$

$$\overset{\Phi_0\text{sym}}{=} -2C_{\text{flip}}\sum_{abij}^{\text{no } t_z}\Bigg[\overbrace{|\langle 10|\eta|10\rangle|^2 + \tfrac{1}{2}|\langle 11|\eta|11\rangle|^2 + \tfrac{1}{2}|\langle 1{-}1|\eta|1{-}1\rangle|^2 - \big(\langle 10|\eta|10\rangle + \langle 00|\eta|00\rangle\big)\big(\langle 11|\eta|11\rangle + \langle 1{-}1|\eta|1{-}1\rangle\big)}^{\text{Isospin conserving}}$$

$$+ \underbrace{\tfrac{1}{2}|\langle 10|\eta|00\rangle|^2 + \tfrac{1}{2}|\langle 00|\eta|10\rangle|^2 - \big(\langle 10|\eta|00\rangle + \langle 00|\eta|10\rangle\big)\big(\langle 11|\eta|11\rangle - \langle 1{-}1|\eta|1{-}1\rangle\big)}_{\text{Isospin mixing}}\Bigg]$$

References

[1] J. C. Hardy and I. S. Towner, Phys. Rev. C **102**, 045501 (2020).

[2] R. W. et al. (Particle Data Group), Progress of Theoretical and Experimental Physics **2022**, 083C01 (2022).

[3] H. Young and R. Freedman, *University Physics with Modern Physics* (Pearson, 2019).

[4] K. S, *Introductory Nuclear Physics* (Wiley India, 2008).

[5] J. Suhonen, *From Nucleons to Nucleus: Concepts of Microscopic Nuclear Theory*, Theoretical and Mathematical Physics (Springer Berlin Heidelberg, 2007).

[6] Lepine-Szily, A. Lépine-Szily, A. Descouvemont, P. Descouvemont, and Pierre, International Journal of Astrobiology **11**, 243 (2012).

[7] P. Marmat, *Equation of state based on phenomenological relativistic mean field theory for single and double fluid neutron stars*, Ph.D. thesis (2022).

[8] P. Cappellaro, Introduction to applied nuclear physics, Massachusetts Institute of Technology: MIT Open-CouseWare, https://ocw.mit.edu/ (Spring 2012).

[9] N. Schwierz, I. Wiedenhover, and A. Volya, Parameterization of the woods-saxon potential for shell-model calculations (2007), arXiv:0709.3525 [nucl-th] .

[10] S. Franchoo, The nuclear shell model (2000).

[11] C. Qi, Sh2011 theoreticl nuclear physics, KTH Royal Institute of Technology (Spring 2015).

[12] I. Shavitt and R. Bartlett, *Many-Body Methods in Chemistry and Physics: MBPT and Coupled-Cluster Theory* (2009).

[13] A. Altland and B. Simons, *Condensed Matter Field Theory*, Cambridge books online (Cambridge University Press, 2010).

[14] D. Griffiths and D. Schroeter, *Introduction to Quantum Mechanics* (Cambridge University Press, 2018).

[15] M. Hjorth-Jensen, M. Lombardo, and U. van Kolck, *An Advanced Course in Computational Nuclear Physics: Bridging the Scales from Quarks to Neutron Stars* (2017).

[16] H. Hergert, Physica Scripta **92**, 023002 (2016).

[17] M. Heinz, A. Tichai, J. Hoppe, K. Hebeler, and A. Schwenk, Phys. Rev. C **103**, 044318 (2021).

[18] T. D. Morris, N. M. Parzuchowski, and S. K. Bogner, Physical Review C **92**, 10.1103/physrevc.92.034331 (2015).

[19] S. R. Stroberg, IMSRG++ (2018).

[20] S. Stroberg, TRIUMF Progress in Ab Initio Nuclear Theory, University of Notre Dame (Feb 28 2023).

[21] V. Cirigliano, Z. Davoudi, J. Engel, R. J. Furnstahl, G. Hagen, U. Heinz, H. Hergert, M. Horoi, C. W. Johnson, A. Lovato, E. Mereghetti, W. Nazarewicz, A. Nicholson, T. Papenbrock, S. Pastore, M. Plumlee, D. R. Phillips, P. E. Shanahan, S. R. Stroberg, F. Viens, A. Walker-Loud, K. A. Wendt, and S. M. Wild, Journal of Physics G: Nuclear and Particle Physics **49**, 120502 (2022).